FEMS Microbiology Ecology, 95, 2019, fiz064

doi: 10.1093/femsec/fiz064
Advance Access Publication Date: 10 May 2019
Research Article

RESEARCH ARTICLE

Sanguina nivaloides and *Sanguina aurantia* gen. et spp. nov. (Chlorophyta): the taxonomy, phylogeny, biogeography and ecology of two newly recognised algae causing red and orange snow

Lenka Procházková[1,*,†], Thomas Leya[2], Heda Křížková[1] and Linda Nedbalová[1,3]

[1]Charles University, Faculty of Science, Department of Ecology, Viničná 7, 128 44 Prague 2, Czech Republic, [2]Fraunhofer Institute for Cell Therapy and Immunology, Branch Bioanalytics and Bioprocesses IZI-BB, Extremophile Research & Biobank CCCryo, Am Muehlenberg 13, 14476 Potsdam-Golm, Germany and [3]The Czech Academy of Sciences, Institute of Botany, Dukelská 135, Třeboň, 379 82, Czech Republic

*Corresponding author: Charles University, Faculty of Science, Department of Ecology, Viničná 7, 128 44, Prague 2, Czech Republic. Tel: +420 221951809; E-mail: lenkacerven@gmail.com

One sentence summary: Red and orange spherical cysts causing snow colouration across several continents were investigated with regards to their geographic distribution, ecology, ultrastructure and phylogeny; the cosmopolitan distribution of a new independent lineage *Sanguina* within the Chlamydomonadales was molecularly confirmed.

†Lenka Procházková, http://orcid.org/0000-0003-3995-6483

ABSTRACT

Melting snowfields in polar and alpine regions often exhibit a red and orange colouration caused by microalgae. The diversity of these organisms is still poorly understood. We applied a polyphasic approach using three molecular markers and light and electron microscopy to investigate spherical cysts sampled from alpine mountains in Europe, North America and South America as well as from both polar regions. Molecular analyses revealed the presence of a single independent lineage within the Chlamydomonadales. The genus *Sanguina* is described, with *Sanguina nivaloides* as its type. It is distinguishable from other red cysts forming alga by the number of cell wall layers, cell size, cell surface morphology and habitat preference. *Sanguina nivaloides* is a diverse species containing a total of 18 haplotypes according to nuclear ribosomal DNA internal transcribed spacer 2, with low nucleotide divergence (≤3.5%). Based on molecular data we demonstrate that it has a cosmopolitan distribution with an absence of geographical structuring, indicating an effective dispersal strategy with the cysts being transported all around the globe, including trans-equatorially. Additionally, *Sanguina aurantia* is described, with small spherical orange cysts often clustered by means of mucilaginous sheaths, and causing orange blooms in snow in subarctic and Arctic regions.

Keywords: snow algae; red snow; haplotype network; *Chlamydomonas nivalis*

Received: 20 December 2018; **Accepted:** 9 May 2019

INTRODUCTION

Several algal species are reported to cause the macroscopic phenomenon of orange and red to pinkish snow, the latter often referred to as 'watermelon snow' or 'blood snow' when occurring as mass developments, including *Chlamydomonas nivalis* (Wille 1903; Kol 1968; Czygan 1970; Fjerdingstad *et al.* 1974; Kawecka 1981; Gradinger and Nürnberg 1996; Leya 2004), *Chloromonas nivalis* (Remias *et al.* 2010; Matsuzaki, Nozaki and Kawachi 2018), *Cr. brevispina* (Hoham, Roemer and Mullet 1979), *Cr. polyptera* (Remias *et al.* 2013), *Cr. rubroleosa* (Ling and Seppelt 1993), *Cr. nivalis* subsp. *tatrae* (Procházková *et al.* 2018a), *Chlorosarcina antarctica* (Ling 2002), *Smithsonimonas abbotii* (Kol 1942), *Chlainomonas kolii* (Novis 2002) and *Chlainomonas rubra* (Hoham 1974).

One of the first field samples of red snow was collected during the Northern Expedition under Captain Ross in August 1818 to Baffin Bay (75°54' N 67°15' W) between northern Greenland and Canada (Bauer 1819) and brought back to England to be investigated. Red snow has been reported from almost all polar and alpine regions (Kol 1968; Marchant 1982; Mataloni and Tesolín 1997; Thomas and Broady 1997). The first phylogenetic studies that identified a separate clade comprising solely red spherical cysts were based on 18S rRNA gene data (Leya 2004; Remias *et al.* 2010, 2013), but a deeper molecular identification based on nuclear ribosomal DNA internal transcribed spacer 2 (ITS2) sequence data so far has been missing for this taxon except for a recent study by Segawa *et al.* (2018) investigating samples from both poles. Red spherical cysts have also been the focus of a few metagenomic studies carried out in the USA (Brown, Ungerer and Jumpponen 2016), Japan (Terashima *et al.* 2017), the Arctic (Lutz *et al.* 2016; Segawa *et al.* 2018) and the Antarctic (Segawa *et al.* 2018). However, detailed investigations of red snow from mid-latitude mountain ranges like those in Europe are lacking.

Though modern microscopes are much better equipped than 200 years ago, a persistent problem is that the red spherical cysts abundantly found in melting snow simply do not reveal enough intracellular details that can be used for a deep morphological description and thus, identification. The unicellular, thick-walled cyst stages ['cysts' = unicellular life cycle stage protected from unfavourable environmental conditions with a wall, which was built exogenously or endogenously according to Ettl and Gärtner (2014)] dominate snow surfaces during summer. The characteristic dark blood-red pigment astaxanthin is accumulated in similarly large quantities only in *Haematococcus lacustris*, *Chlainomonas rubra* and some others (Remias, Lütz-Meindl and Lütz 2005). In many cases astaxanthin covers the cysts' chloroplast structure almost entirely, making light microscopy hardly illuminating. A first revision of *Chlamydomonas* by Pröschold *et al.* (2001) revealed how important chloroplast morphology is for consistency with the phylogeny of the Chlamydomonadaceae. Many snow algal species are held as live cultures in culture collections (e.g. CCCryo, UTEX, CCAP), but none of these 'green' species ever formed a single phylogenetic clade together with red spherical cysts from red snow. Instead, all 18S rRNA gene phylogenetic studies have revealed a single clade comprising immotile spherical red cysts (Leya 2004; Leya, Müller, Ling *et al.* 2004; Remias *et al.* 2010, 2013). This 'red snow' clade is clearly separated from other clades of *Chlamydomonas, Chloromonas, Lobochlamys, Oogamochlamys, Haematococcus, Carteria*, etc. Most likely, green, flagellated isolates from red snow field samples often were misinterpreted as having resulted from red spherical cysts or even vice versa; e.g. Novakovskaya *et al.* (2018) thought to have observed such a phenomenon when linking green isolates of *Cr. reticulata* from snow samples to red cysts in the same sample. The lack of knowledge about other life cycle stages, whether vegetative (e.g. green actively dividing cells with a well-visible chloroplast) or sexual (e.g. gametes), and the lack of sufficient molecular data from red spherical cysts, have been the most hindering in identifying their true taxonomy.

In this study we used a polyphasic approach to study field material composed of spherical red and orange cysts sampled from alpine habitats in Europe, North America, South America and both polar regions. Our aims were (i) to reveal their molecular diversity based on ITS2 rDNA and rbcL gene sequences, (ii) to describe their morphological and ultrastructural cellular details using light, transmission and scanning electron microscopy, and (iii) to characterise their habitat conditions (pH, conductivity, elevation). Furthermore, we wanted (iv) to describe the geographic distribution of haplotypes detected by establishing a haplotype network, and (v) to test the existence of spatial patterns (Mantel test, sPCA). Based on the results, a new genus-level taxonomy of the examined species is proposed with a description of two new species: the new genus *Sanguina* Leya, Procházková et Nedbalová with *Sanguina nivaloides* Procházková, Leya et Nedbalová and *Sanguina aurantia* Leya, Procházková et Nedbalová.

MATERIALS AND METHODS

Sampling localities

Patches of clearly visible red- or orange-coloured snow caused by spherical red or orange cells were collected from 42 localities in melting seasons between the years 1999 and 2018 (Fig. 1, Supplementary Tables 1 and 2): 22 samples originated from alpine sites in continental Europe, three from sites in North America and one from South America. Moreover, 14 samples were collected at polar sites on the island of Spitsbergen (Svalbard archipelago) and two from polar sites on the Antarctic Peninsula.

To ensure the selection of 'clean' (mono-specific) bloom spots and to avoid a taxonomically diverse sample, a field microscope was used to check the sample in the field before collection. In the lab, samples were further thoroughly examined using laboratory light microscopy (see below) prior to molecular analyses. If the sample appeared to be too diverse, it was discarded. In addition, Alanagreh *et al.* (2017) reported that the dominant haplotype was usually evident from the Sanger sequencing, similar as in cloning approach.

Measurements of pH and conductivity and snow water equivalent (referred to as 'snow water content' in the paper cited) were carried out according to Procházková *et al.* (2018a).

In addition we were also able to investigate red cysts collected in 1851, namely from the desiccated sample 'MB_ES_1781c', further labelled 'Rother Schnee Crimsen [*sic*] Cliff Beverly 1851, 76°3'N.B. 1781c' obtained from the Ehrenberg Collection at the Museum für Naturkunde in Berlin. This historical material was collected during the Grinnel Arctic Expedition (1850–1851) under Lieut. De Haven of the U.S. American Marines from red snow on scarlet-coloured cliffs (Crimson Cliffs) in Baffin Bay on the Greenland coast (Beverly Greenland), though a bit further north of the location, from where the Ross type sample of 1818 originated (75°54' N 67°15' W; Ross 1820). Unfortunately, the latter material was not traceable and could not be included in this study.

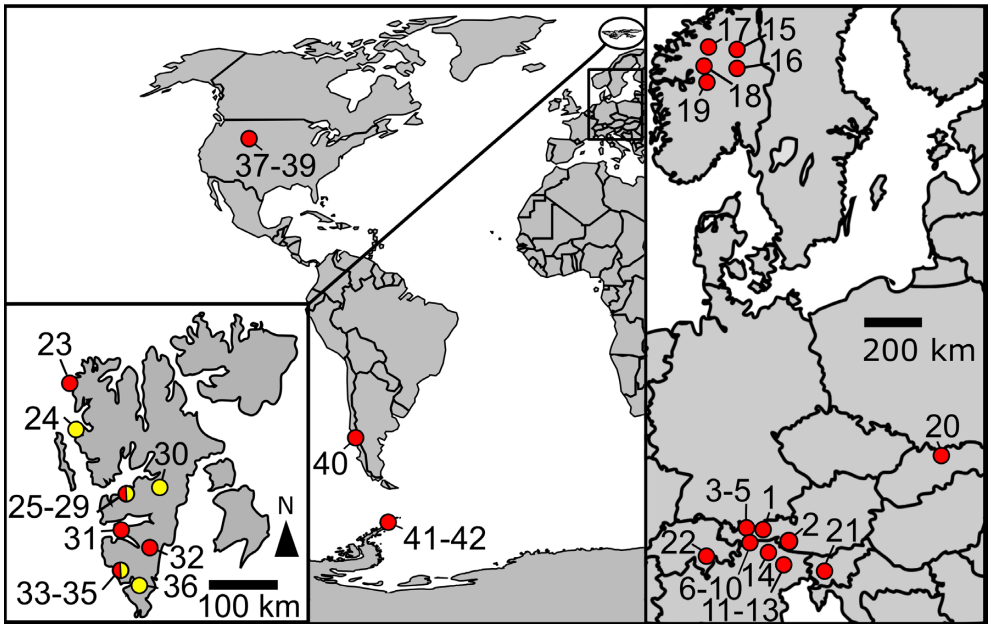

Figure 1. Sampling locations of *Sanguina nivaloides* (red circles), *Sanguina aurantia* (yellow circles) and regions where both species were sampled (red-yellow circles) in continental Europe (right), on the archipelago of Svalbard (left), in North and South America (middle) and in Antarctica (middle). Numbering corresponds to the sample origin from the following countries: Austria (1–10; 1-Haferkarlespitze, 2-High Tauern, 3–5 Kühtai, 6–10 Ötztal Alps), Italy (11–14; 11–13 Dolomites, 14-Sarntal Alps), Norway (15–19), Slovakia (20-High Tatra Mountains), Slovenia (21-Julien Alps), Switzerland (22-Urner Alps), Svalbard (Norway) (23–36; 23-Amsterdamøya, 24-Ny Ålesund, 25–29 Longyearbyen, 30-Raggfjellet, 31-Midterhuken, 32-Doktorbreen, 33–35 Hornsund, 36-Chomjakovbreen), Colorado (USA) (37–39 Rocky Mountains), Argentina (40-Patagonia), Antarctica (41–42 Antarctic Peninsula). Habitat description of sampling localities including geographical data are shown in Supplementary Table 1.

Light and electron microscopy

Light microscopy was performed using an Olympus BX43 (Olympus Corporation, Japan) equipped with a DXM 1200F digital camera (Nikon, USA). Microphotographs were further processed using the QuickPHOTO Camera 3.0 software (Promicra, Czech Republic). The same software or cell^P software (version 3.4, Olympus Soft Imaging Solutions GmbH, Germany) was used to measure cell sizes. Preparation of samples for scanning and transmission electron microscopy (SEM and TEM) followed the protocol described in Procházková *et al.* (2018a). The diameters of around 40 cysts were measured for each field sample. Measurements of red cysts from 1851 from the desiccated sample 'MB_ES_1781c' were also included.

DNA extraction and PCR

DNA isolation was carried out using the DNeasy Plant Mini Kit (Qiagen, Germany) as described in Procházková *et al.* (2018a). If less than 20 mg wet biomass was available, DNA was extracted using the Instagene Matrix (Bio-Rad Laboratories, USA) according to Remias *et al.* (2016). The 18S small subunit ribosomal RNA gene (18S rRNA gene), internal transcribed spacer region 2 (ITS2 rDNA) and ribulose-1,5-bisphosphate carboxylase/oxygenase large subunit (rbcL) gene regions were amplified from DNA by polymerase chain reaction (PCR) using the primers listed in Supplementary Table 3. Primer pairs involved in the PCR of 18S were P2/P4, 18F2/18R2, FC/RF and FA/RD. In order to amplify ITS2 we used ITS1/ITS4, ITS5/ITS4, SSU/LSU, Al1500af/LR3 and TW81/AB28. For PCR of rbcL, we used the primer pairs rbcL1F/rbcL7R, rbcL1F/rbcL4R, rbcL10F/rbcL7R, rbcL8F/rbcL7R, Snow-F3/Snow-R12 and Snow-F0/Snow-R12. The amplification reactions for these markers are described in Procházková *et al.* (2018a). PCR products were purified and sequenced using an Applied Biosystems automated sequencer (ABI 3730xl) at Macrogen (Netherlands). Chromatograms of all newly obtained sequences were carefully examined using the program FinchTV 1.4.0 (Geospiza, USA). Only sequences showing distinct single peaks in the electropherogram were used. The nuclear rDNA ITS2 region was identified using a web interface for the ITS2 database showing the position of the 26S motif (http://its2.bioapps.biozentrum.uniwuerzburg.de/cgi-bin/index.pl?annotator; Koetschan *et al.* 2010). The sequences obtained were submitted to the NIH genetic sequence database GenBank at NCBI (accession numbers are shown in Supplementary Tables 4–6).

Molecular analyses

Our 18S rRNA gene alignment contained 96 sequences (1544 bp) and the rbcL matrix consisted of 62 sequences (954 bp); members of *Chaetophora*-clade were selected as the outgroup. The best-fit nucleotide substitution model was estimated by jModeltest 2.0.1 (Posada 2008). Based on the Akaike Information Criterion (AIC), the TIM2+I+G model was selected for the 18S rRNA gene. Three partitions were set for rbcL gene sequences and the following substitution models were applied: GTR+I+G (1st codon position), TIM3+I (2nd codon position) and GTR+I+G (3rd codon position). The 18S rRNA gene and rbcL phylogenetic trees were inferred by Bayesian Inference (BI) and Maximum Likelihood (ML) according to Nedbalová *et al.* (2017), with the minor modification that Markov Chain Monte Carlo runs were carried out for three million generations in BI. Convergence of the two cold chains was checked by the average standard deviation of split frequencies (0.000014 and 0.001613 for the 18S rRNA gene and rbcL dataset, respectively). Bootstrap analyses were performed by maximum likelihood and Bayesian posterior probabilities were calculated as described by Nedbalová *et al.* (2017).

The 42 sequences of ITS2 rDNA obtained during this study were used as the main dataset which was split into a red snow dataset (35 sequences) and an orange snow dataset (seven sequences). The extended dataset additionally included selected published sequences, which were assigned to the investigated species based on a pairwise comparison using BLAST. The newly generated ITS2 sequences of our red snow sample RS_0015–2010 (accession number MK728599) and orange snow sample RS_0017–2010 (accession number MK728634) were used as a query. Samples of these additional sequences originated from Colorado and Washington states (USA) (NCBI accession codes KX063716.1-KX063729.1 and KX063743.1-KX063753.1; Brown, Ungerer and Jumpponen 2016), and from Alaska (AB902998.1), Greenland (AB902971.1), the Austrian Alps (GU117577.1; Remias *et al.* 2010) Japan (AB903028.1) and Tadjikistan (AB902973.1, AB903025.1). The individual sequences of specimens with ambiguous positions (one or two ambiguous bases out of 205 bp in these specimens from the main dataset: redCol, 4HT, 2SLOV, 4D, 9D; one or eight ambiguous bases out of 205 bp in specimens of the extended dataset: AL1, JP1) were resolved using the PHASE algorithm implemented in DnaSP v.6.0. (Librado and Rozas 2009). PHASE assumes Hardy-Weinberg equilibrium and uses a coalescent-based Bayesian method to infer haplotypes (Librado and Rozas 2009). This means the PHASE algorithm can successfully infer haplotypes if a sufficiently high number of homozygotic sequences are used. All samples were resolved with a strong support. Haplotypes were delineated at the 100% similarity threshold (i.e. two sequences belong to the same haplotype if they are identical). Only different haplotypes were used in the ITS2 secondary structure modelling, whereas all haplotypes were used in the ITS2 haplotype network analysis. For the ITS2 haplotype network of a species causing red snow the main dataset and extended dataset consisted of 40 and 59 sequences, respectively. For the ITS2 haplotype network of a species causing orange snow the main dataset and extended dataset consisted of seven and 21 sequences, respectively.

The ITS2 rDNA sequences were folded using the Mfold server at http://mfold.rna.albany.edu/?q5mfold (Zuker 2003). The secondary structure model that was consistent with the following specific features of the nuclear rDNA ITS2 was selected, namely four helices and a U–U mismatch in helix II (Coleman 2007). The ITS2 sequences were aligned on the basis of the sequence-structure analysis (Schultz and Wolf 2009) using the 4SALE tool (Seibel *et al.* 2006, 2008). At this step a manual validation and correction of the sequence alignment and secondary structure was necessary. The alignments of the main and the extended dataset included 213 bp and both were used in the consensus secondary structure modelling and haplotype network. The secondary structure of the nuclear rDNA ITS2 of specimen RS_0015–2010 (accession number MK728599) was drawn using Visualization Applet for RNA (VARNA) version 3.9 (Darty, Denise and Ponty 2009). The consensus secondary structure was edited using Inkscape software version 0.91 (Free Software Foundation Inc., USA). The number of compensatory base changes (CBC; a double-sided base change of a nucleotide pair in a helix, retaining the secondary structure) between haplotypes was evaluated using the 4SALE tool. The nuclear network for ITS2 was constructed by TCS software version 1.21 (Clement, Posada and Crandall 2000) using statistic parsimony under a 95% connection limit. Then we ran a second analysis, reducing the connection limit to 91% in an attempt to infer connections among subnetworks. Gaps were considered the fifth phylogenetic character (Vukić, Ulqini and Šanda 2017). The final edit of the haplotype network was again carried out in Inkscape.

Geographic relationships

To investigate the spatial genetic structure of the red snow alga studied, we summarised genotype allele frequency data of the variable ITS2 rDNA marker by performing a spatial principal component analysis (sPCA). A principal component analysis (PCA) summarises multivariate genetic information into a few linearly uncorrelated variables, the principal components (Jombart, Pontier and Dufour 2009). The PCA method was recently modified to include spatial information to investigate the part of the genetic variation that is or is not spatially structured, the sPCA (Jombart *et al.* 2008). The sPCA analyses a matrix of relative allele frequencies, which contains genotypes in rows and alleles in columns. Geographic coordinates of sampling points are used as input data for the creation of a list of weights derived from a connection network (function 'chooseCN'). Our sPCAs were performed with the *adegenet* package in R software (Jombart 2008), and using the function 'spca' and bar plots of the sPCA eigenvalues were produced showing the amount of genetic diversity (as measured by the multivariate method being used) represented by each principal component. To test for the existence of global and/or local structure, we performed two Monte Carlo multivariate tests (Jombart *et al.* 2008). The outputs are represented as figures showing two histograms (one for the global test and one for the local test) of permuted test statistics, and the reference distribution of these statistics is obtained by randomly permuting the rows of the genotype datamatrix. Spatial PCA was carried out for two versions of the datasets of the red spherical cysts: (i) Europe, America, Antarctica and Svalbard, and (ii) Europe. To assess the significance of the correlation between ITS2-based genetic and geographic distance matrices of the investigated species causing red snow, we also performed a classical Mantel test ('mantel.randtest') using the package *adegenet* in the R software. Pairwise Euclidean distances for both distance matrices were computed using the function 'dist'. Haplotype diversity of the species studied within and among mountain ranges (European Alps, Tatra Mountains, continental Norway, Svalbard, Rocky Mountains, Patagonia) and polar regions (Svalbard, Antarctica) were evaluated using the program MEGA (version 7.0.14); genetic distances between ITS2 sequences were generated using both uncorrected (p-distance) and corrected pairwise distance [Kimura two-parameter (K2P) distance]. The number of base differences, uncorrected (p-distance) and corrected pairwise distance (K2P) between 18 ITS2 haplotypes of red cysts and two ITS2 haplotypes of orange cysts were evaluated with MEGA as well.

RESULTS

Habitat conditions

The species causing red snow in this study, *Sanguina nivaloides*, occurred on temporary (alpine meadows, polar rocks, permafrost) or persistent (glaciers) snowfields in both alpine and polar regions (Supplementary Fig. 1). This species was hardly found at mountain sites below the timber line (e.g. sample 'subalpine'). It was observed occasionally in massive amounts on open icy glacier surfaces, though as long as there is a snow layer on the glacier, this habitat is also occupied. The species causing orange snow in this study, *Sanguina aurantia*, occurred at similar habitats on Svalbard only. At localities where these species

are found once, they appear consistently year after year, forming reddish or orange blooms in summer, producing the well-known macroscopic phenomenon of red snow or blood snow due to the dominating red pigment astaxanthin in its cysts. Colour shades can vary from orange (orange spherical cysts) and pink to dark cherry and blood red (red spherical cysts) (Supplementary Fig. 2). These localities are usually well-defined in their extent and can cover areas from a few square metres up to several hundreds of square metres. Over summer and with melting of the snow cover algal populations are slowly exposed on the snow surface, and are often washed down from snow fields in alpine regions, resulting in intensely coloured streaks on the otherwise white snow. If a snow field is not persistent over the summer months, the cysts can end up on permafrost or rocky soil, and then covered by fresh snow at the end of the summer. There they are a 'seed bank' serving as an inoculum for the next melting season when the newly encountered habitat is suitable. In addition, they may be dispersed to other locations by strong winds or storms, which are e.g. typical for autumn in the polar region around Svalbard. Snow fields with blooms of *Sanguina nivaloides* can be almost flat or be part of a steep slope, with any variation in between. Blooms have been observed at sites close to alpine pathways and on pastures, as well as at polar sites far away from any signs of civilisation, e.g. on remote inland glaciers on Spitsbergen. Also, organic nutrient input was not a decisive factor, as we found red snow both far away and also close to bird colonies. Red snowfields were located at elevations between 13 and 585 m a.s.l. in polar regions, and between 1914 and 3731 m a.s.l. in alpine regions (Supplementary Table 1). The orange snowfields were located between 10 and 500 m a.s.l. in polar regions (Supplementary Table 2). In snowfields with *S. nivaloides* or *S. aurantia*, blooms had low electrical conductivities (3–26 μS cm^{-1}, occasionally up to 84, but usually well below 100 μS cm^{-1}) and pH values between slightly acidic (pH 4.7) and neutral (pH 7.1) (Supplementary Tables 1 and 2). Snow temperatures were naturally stable near 0°C. The water equivalent of a red blooming snowfield in the Austrian Alps amounted to 51.6 ± 1.6% (sample WP123). Snow field inclination and its cardinal direction towards the sun are thought to account for decisive differences in incident solar radiation and temperature, but neither were correlated with the occurrence of red snow.

Cytological observations

Light microscopy (Fig. 2) and electron microscopy (SEM: Fig. 3, TEM: Fig. 4) showed that field samples of *Sanguina nivaloides* consisted of red spherical cells exhibiting different accumulation levels of secondary carotenoids in abundant lipid droplets, which in mature cysts fully masked the chloroplasts making any detailed structure unrecognisable by light microscopy (Fig. 2A) and thus unusable for identification. A single parietal chloroplast and one or two large, unpigmented vacuoles were observed in young cells in their early stage of development only (Fig. 2B–D and Fig. 4C and D). The typical mature red cyst was smooth-walled (Figs 2A and 3A), but in two cases the red snow also consisted of populations of cysts with nipples (Figs 2E, 3B and 4F). A few scattered cysts with short blunt nibs (Fig. 3C) or pronounced papillae (Figs 2F and 3D) or cells carrying uniformly distributed small smooth papillae (Fig. 3E) were noticed in a population of smooth-walled cells . *Sanguina aurantia* field samples (Fig. 5) consisted of smaller spherical cysts with a striking orange-coloured cell content, the cells had an outer distant cell layer or the distant layer was absent. A few scattered cells of 'ruby'-like cysts (the term 'ruby' is frequently used for this type of cyst as the dark red pigmented cyst content and the wall structure appear like a ruby encased in mother-of-pearl) were found in two red snow samples (Supplementary Fig. 3A-F, marked with an asterisk in Supplementary Table 4). We are certain that no sequences of those ruby cysts were used in any of the analyses in this study, as they would have been greatly outnumbered by the dominating smooth-walled cysts, even assuming they were equally amenable to DNA extraction in the first place. As far as the intracellular ultrastructure of our samples is concerned, mature cysts had a naked pyrenoid in a single chloroplast, which is forced into a central position by surrounding lipid globules (Fig. 4A) and cell walls consisted of two layers (Fig. 4B). Early stages of red cysts differed in the presence of a clearly visible single parietal chloroplast (Fig. 4C and D) and a three-layered cell wall, the outermost being fuzzy (Fig. 4E). Orange-coloured cysts of *Sanguina aurantia* differed from red cysts of *Sanguina nivaloides* in the structure of the second layer of their cell wall, being multilayered and slightly undulating on the surface (Fig. 5C and E). This layer most likely reflects the maturity of the cysts, as orange-coloured cysts of the same cell diameter but with smooth surfaces also existed in this population of *Sanguina aurantia* (Fig. 5D). Cytosolic electron-dense vacuoles filled with a crystalline structure were observed in both red cysts of *Sanguina nivaloides* and in orange-coloured cysts of *Sanguina aurantia* (Fig. 5G).

Size ranges of the orange-coloured cysts and red cysts overlapped, with 6.2–15.5 μm and 7.3–39.0 μm, respectively. The variability of cell size ranges in field samples of each haplotype of both snow algal species (for description see below) is shown in Supplementary Fig. 4. The material from Baffin Bay (sample 'MB_ES_1781c' from the Ehrenberg Collection at the Museum für Naturkunde in Berlin) contained cells in the size range typical for red cysts (Fig. 6).

Molecular identification of genus *Sanguina* and its closest relatives

According to our 18S rRNA gene and rbcL phylogenies (Figs 7 and 8), the genus *Sanguina* forms a monophyletic lineage within the Chlamydomonadaceae containing samples from nearly all regions of the Earth (Greenland, North America, South America, Africa, Europe, Asia, Svalbard and Antarctica). The closest relatives to the genus *Sanguina* are organisms found on glaciers or glacier-associated environments, such as the strain CCCryo 086–99 (cf. *Ploeotila* sp.) from a glacier surface or uncultured eukaryote clones from glacial debris in Alaska and periglacial environments on the top of Mount Kilimanjaro in Tanzania. Slightly distant relatives represent strains from the Arctic permafrost in close vicinity to glaciers and snow fields, e.g. CCCryo 101–99 and CCCryo 133–01 (both cf. *Sphaerocystis* sp.) or Arctic snow fields, e.g. CCCryo 147–01 (cf. *Coenochloris* sp.), and from soil such as 'uncultured Haematococcaceae clones' isolated from an aspen rhizosphere and *Gloeocystis* sp. from desert soil in Washington State. Phylogeny based on rbcL data (Fig. 8) showed an increased molecular variability in comparison with 18S rRNA gene data among specimens of the genus *Sanguina* because of the degeneracy of the genetic code, which accounts for the existence of synonymous mutations. Interestingly, the small orange cysts of *Sanguina aurantia* formed a small subclade within the red cyst samples of *Sanguina nivaloides*. The rbcL phylogeny confirmed the positions of cf. *Sphaerocystis* and cf. *Coenochloris* as slightly distant relatives to *Sanguina nivaloides*. Additionally, it revealed that these genera form closely related lineages (Fig. 8) to *Achoma brachiatum* isolated from an alpine herbfield soil in New

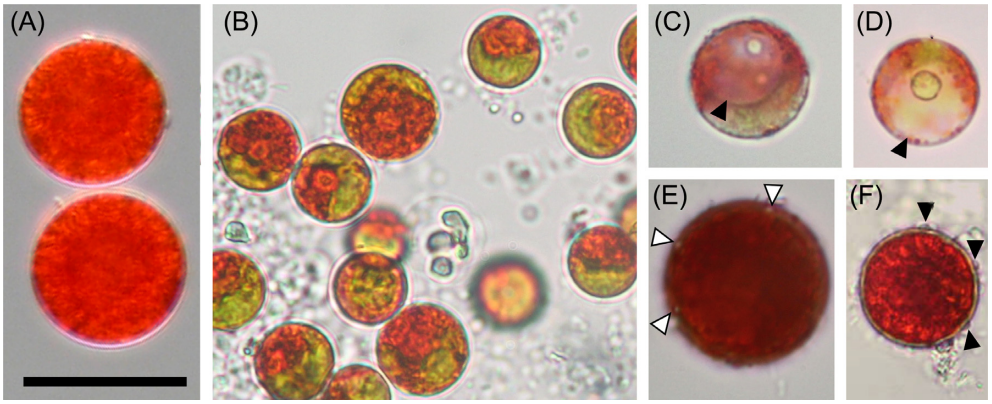

Figure 2. Light microphotographs of *Sanguina nivaloides*. **(A)** Typical mature red cyst with smooth cell wall (holotype specimen CCCryo RS_0015–2010), abundant lipid droplets entirely masking the cell interior and structure of the chloroplast. **(B-D)** Young red cysts in early stage of development, (B) showing visible parts of a single parietal chloroplast (paratype sample WP123), (C-D) depicting the large unpigmented vacuole (arrowhead) (samples: Sva4 and Saddle). **(E-F)** Mature red cysts of less frequent haplotypes causing red blooms, (E) visualises nipples on the cell surface (arrowheads, paratype specimen CCCryo RS_0003–2004). (F) shows pronounced papillae on cell surface (arrowheads, sample 4D). Scale bar 20 μm.

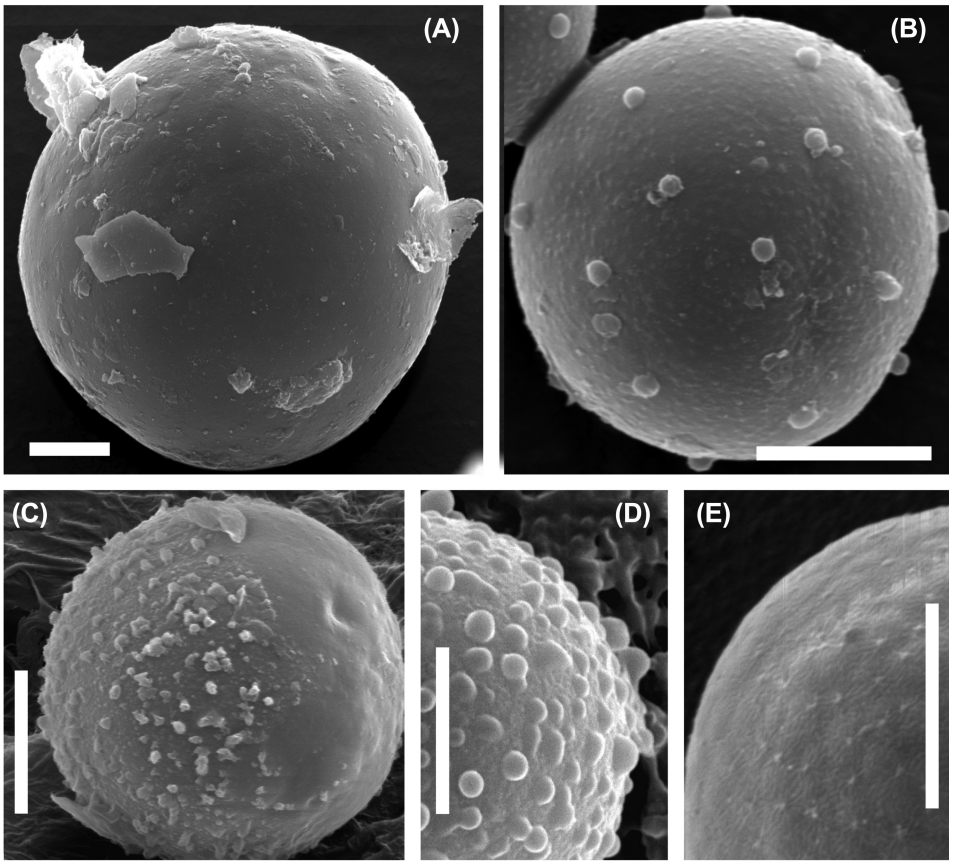

Figure 3. Scanning electron microphotographs of *Sanguina nivaloides*. **(A)** Typical mature red cyst with smooth cell wall (holotype specimen RS_0015–2010). **(B-D)** Mature red cysts of less frequent haplotypes causing blooms, (B) showing nipples on cell surface (paratype specimen RS_0003–2004), (C) depicts the smooth surface with short blunt nibs, which may represent the compressed remnants of the presumably transient primary cell wall, this cell wall layer may decompose over time (note: on the left side of the cell 'papillae' are present, on the right side they are absent, specimen RS_0011), (D) shows the pronounced papillae on the cell surface (sample 4D). **(E)** Scattered cells with small papillae on their cell surfaces in a population of smooth-walled cells (sample redCol). Scale bars 5 μm.

Zealand (Novis and Visnovsky 2012). Whether any of them could be assigned to the genus *Achoma* is discussed further below, but remains to be investigated. To sum up, the monophyly of the *Sanguina*-clade and the phylogenetic positions of its closest known culturable relatives were confirmed for both markers (Supplementary Figs 5 and 6). Moreover, our phylogenetic analyses demonstrate that the positions of strains SAG 26.86 of *Cr. typhlos* (= UTEX 1969 = CCCryo 122–00), and *Cr. reticulata* SAG 29.83 (= UTEX 1970 = CCCryo 213–05) in the *Chloromonas*-clade based on 18S rRNA gene and rbcL phylogenetic trees clearly differed from the position of *S. nivaloides* (Supplementary Figs 5 and

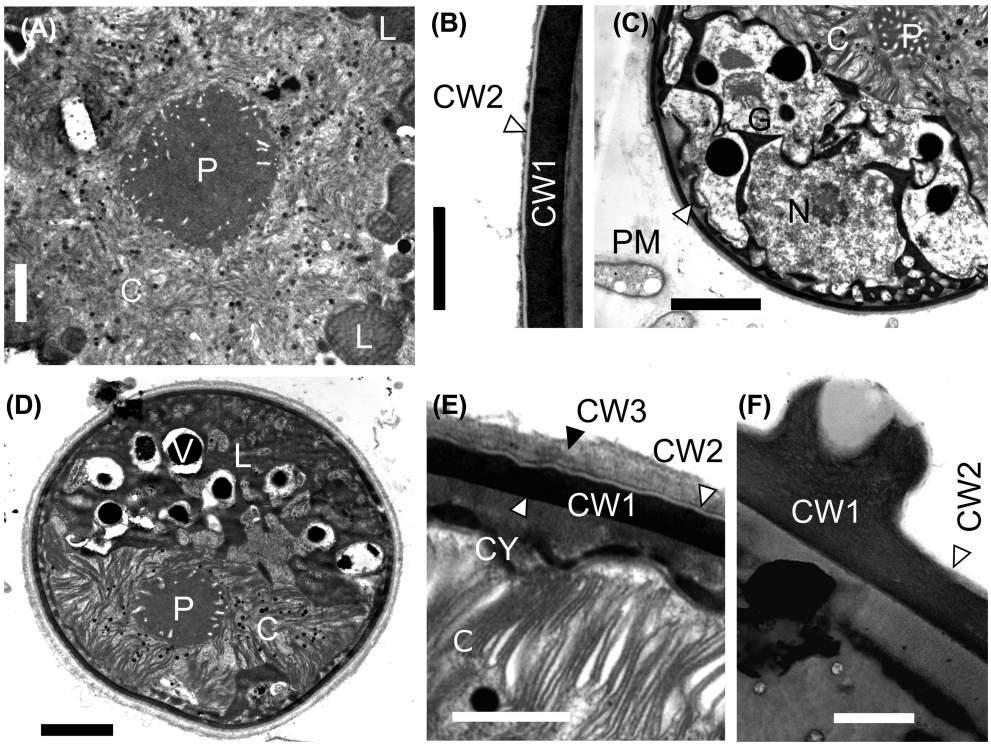

Figure 4. Transmission electron microphotographs of *Sanguina nivaloides*. **(A, B)** Mature red cyst (holotype specimen RS_0015–2010), (A) shows the centrally located plastid with a naked pyrenoid, surrounded by abundant lipid droplets. (B) depicts the electron-dense thick cell wall covered with a very thin transparent layer. **(C-E)** Young red cyst (paratype sample WP123), (C) shows the large cytoplasmatic-free area (arrowhead) between the cytoplasmatic membrane and the cell wall, the nucleus and the parietal plastid, as well as parts of the Golgi aparatus, no lipid bodies visible, (D) depicts the parietal plastid with a naked pyrenoid, lipid bodies and vacuoles, (E) shows a detail of the cell wall consisting of three layers: the innermost—thick electron dense (CW1), the middle one—very thin electron transparent (CW2; trilaminar sheath) and the fuzzy upper layer (CW3; presumably the primary cell wall). **(F)** A detail of a cell wall nipple of less frequent haplotypes (paratype specimen RS 0003–2004). C = chloroplast, CY = cytoplasm, CW1 = cell wall 1, CW2 = cell wall 2, G = Golgi stacks, L = lipid globules, N = nucleus, P = pyrenoid, PM = plasmatic membrane, V = vacuole. Scale bars = 2 μm for (A, C, D). Scale bars = 0.5 μm for (B, E, F).

6). These strains were isolated from snow samples and were formerly believed to cause red snow, and thus, they originally were (mis)identified as *Cd. nivalis* and *Cd. yellowstonensis* (Sutton 1970), respectively. The former is still listed under two different names, as *Cr. typhlos* (SAG) and *Cd. augustae* (UTEX), as is the latter, *Cr. reticulata* (SAG) and *Cr. clathrata* (UTEX); in both cases the designations at SAG are correct. Moreover, strain CCAP 11/128 (= UTEX 2824 = CPCC 528 = CCCryo 214–05; accession number HQ404886.1) is listed as *Cd. nivalis* at UTEX (and others), but in our phylogeny proved to be *Cr. typhlos* based on the comparison of its ITS2 sequences (pairwise blast search), with 100% identity and no CBC for this marker with CCCryo 122–00 of *Cr. typhlos* (= SAG 26.86 = UTEX 1969 = CCAP 11/51B = IAM C-263 = NIES 2226 = IU 1969 [original deposition]; accession number HQ404869.1).

The CBC species concept applied to *Sanguina nivaloides* and *Sanguina aurantia*

The network analysis of field samples of *Sanguina nivaloides* from Europe, North America, South America and Antarctica (35 specimens) applying a 95% connection limit resulted in a total of 18 ITS2 haplotypes interconnected in one network (Fig. 9). Haplotypes differed by one up to seven nucleotide changes out of 205 base pairs (Table 1). The network analysis of *Sanguina aurantia* field samples from Svalbard (seven specimens) resulted in two ITS2 haplotypes differing by one nucleotide change out of 213 bp. Based on the comparison of ITS2 rDNA secondary structures, one CBC was found between *Sanguina nivaloides* (the red cysts) and *Sanguina aurantia* (the small orange cysts) at the 13th position in helix II (Fig. 10). However, there is no consensus as to whether the CBC detected at this position can be used for a species separation within the Chlorophyceae. In other words, some authors treat this position as a variable one (e.g. Demchenko *et al.* 2012), others as a conservative one (e.g. Caisová, Marin and Melkonian 2013). Most recently, CBCs in the 5´ end of helix III were only treated as relevant for evaluating species boundaries between closely related taxa (Segawa *et al.* 2018). Sequence identities between red cysts and small orange cysts were ≥95.1%, whereas sequence identities within red cysts were ≥96.5% (Supplementary Table 7), suggesting that both types of cysts investigated in this study are very closely related. Among the red cysts of *Sanguina nivaloides* no CBC was found in the conserved parts of this marker structure, suggesting that according to the CBC species concept as proposed by Coleman (2000), all our samples of red snow from Europe, North America, South America and Antarctica were caused by one species. The presence of the one CBC and the number of base differences between ITS2 haplotypes of *Sanguina nivaloides* (red cysts) and *Sanguina aurantia* (orange cysts) are summarised in Table 1. Interestingly, two haplotypes of red cysts (H4 and H5) lack the CBC at the 13th position in helix II in their ITS2 secondary structure when compared to small orange cysts (Table 1). When comparing three molecular markers, the lowest intraspecific variability between *S. nivaloides* and *S. aurantia* haplotypes was detected in 18S (≤0.2%), was higher in rbcL (≤4.4%) and the highest was in ITS2 (≤4.9%) (Supplementary Tables 7–9).

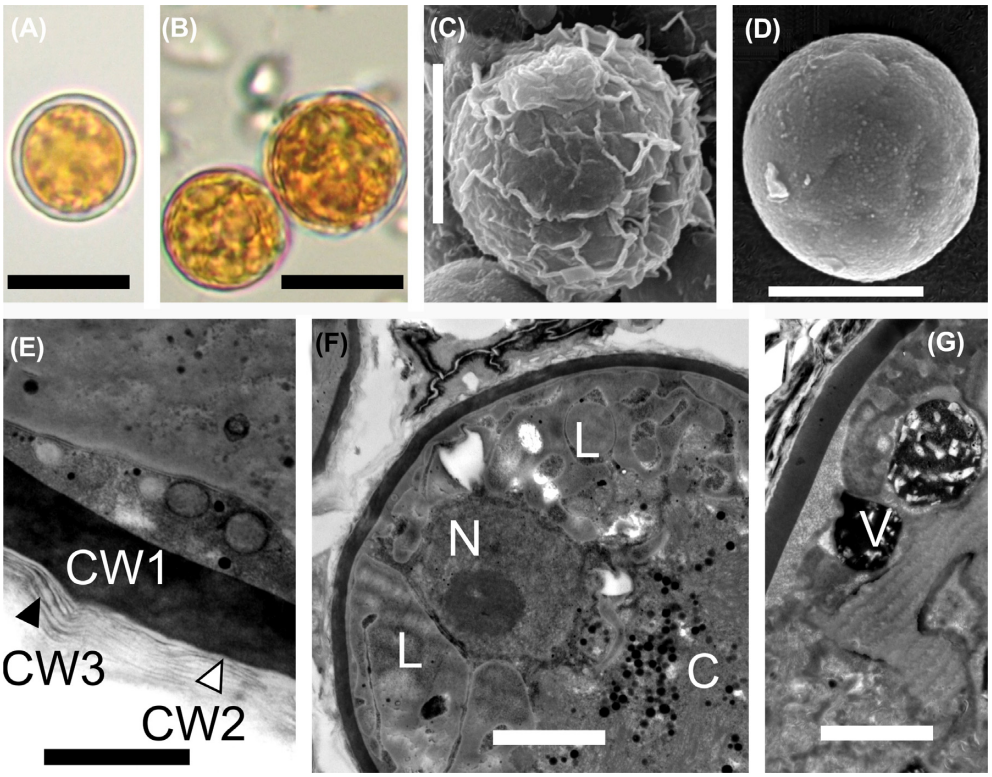

Figure 5. Light and electron micrographs of *Sanguina aurantia* (holotype specimen RS.0017–2010), **(A)** depicts the distant outer cell layer. **(B)** shows that the distant cell layer is absent. **(C-D)** outermost layer is wrinkled and when it is decomposed, the smooth cell wall below may appear. **(E)** shows details of the cell wall with the electron-dense layer (CW1) being covered by several more or less undulating thin transparent layers (CW2, CW3). **(F)** shows a cross-section of the cyst showing the nucleus and the centrally compressed chloroplast. **(G)** depicts the cytosolic electron-dense vacuoles filled with crystalline structures. C = chloroplast, CW1 = cell wall 1, CW2 = cell wall 2, CW = cell wall 3, L = lipid globules, N = nucleus, V = vacuole. Scale bars = 10 μm for (A, B), 5 μm for (C, D), 0.5 μm for (E) and 2 μm for (F, G).

Table 1. Amount of compensatory base changes in the ITS2 secondary structure (lower left) and the number of base differences/number of indels (each of two bp length) (upper right; e.g. '3/4' means that 3 differences and 4 indels were found) between 18 haplotypes of *Sanguina nivaloides* (H1-H18) and two haplotypes of *Sanguina aurantia* (HA1, HA2).

	H1	H2	H3	H4	H5	H6	H7	H8	H9	H10	H11	H12	H13	H14	H15	H16	H17	H18	HA1	HA2
H1		1	2	1	5	4	2	2	3	1	2	3	2	3	3	4	3	3	3/4	4/4
H2	0		1	2	4	5	3	1	2	2	1	2	3	2	2	3	2	2	2/4	3/4
H3	0	0		3	5	6	4	2	3	3	2	3	4	3	3	4	3	3	3/4	4/4
H4	0	0	0		6	5	3	3	4	2	3	4	3	4	3	4	4	4	4/4	5/4
H5	0	0	0	0		7	5	3	6	6	5	6	7	6	6	7	3	6	4/4	5/4
H6	0	0	0	0	0		2	4	5	5	5	6	6	6	6	7	5	6	6/4	5/4
H7	0	0	0	0	0	0		2	5	3	3	4	4	4	4	5	3	4	5/4	6/4
H8	0	0	0	0	0	0	0		3	3	2	3	4	3	3	4	1	3	3/4	4/4
H9	0	0	0	0	0	0	0	0		4	3	4	5	4	4	5	4	4	4/4	3/4
H10	0	0	0	0	0	0	0	0	0		3	4	3	4	4	5	4	4	4/4	5/4
H11	0	0	0	0	0	0	0	0	0	0		1	4	1	1	2	3	1	3/4	4/4
H12	0	0	0	0	0	0	0	0	0	0	0		5	2	2	3	4	2	4/4	5/4
H13	0	0	0	0	0	0	0	0	0	0	0	0		5	5	6	5	5	5/4	6/4
H14	0	0	0	0	0	0	0	0	0	0	0	0	0		2	3	4	1	4/4	5/4
H15	0	0	0	0	0	0	0	0	0	0	0	0	0	0		1	4	2	4/4	5/4
H16	0	0	0	0	0	0	0	0	0	0	0	0	0	0	0		5	3	5/4	6/4
H17	0	0	0	0	0	0	0	0	0	0	0	0	0	0	0	0		4	4/4	5/4
H18	0	0	0	0	0	0	0	0	0	0	0	0	0	0	0	0	0		4/4	5/4
HA1	1	1	1	0	0	1	1	1	1	1	1	1	1	1	1	1	1	1		1
HA2	1	1	1	0	0	1	1	1	1	1	1	1	1	1	1	1	1	1	0	

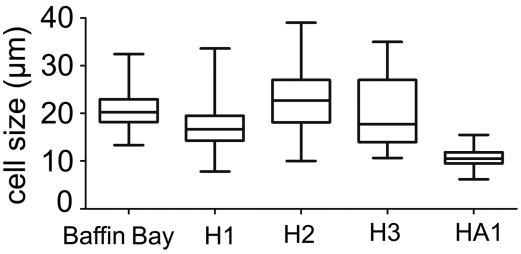

Figure 6. Cell size ranges of cysts of the most common haplotypes of *Sanguina nivaloides* (H1 and H2 = red cysts with smooth cell wall, H3 = red cysts with nipples) and *Sanguina aurantia* (HA1 = small orange cysts) in the dataset studied compared with cell sizes from the Crimson Cliffs in Baffin Bay on Greenland (specimen MB_ES_1781c) (Ehrenberg 1851; Leya 2008).

The geographic distribution of ITS2 haplotypes

For *Sanguina nivaloides* (red cysts), the most frequent haplotype of this study (H1) was found in the High Tatra Mountains (Slovakia), the Swiss Alps (Switzerland), the High Tauern (Austria), Tyrol (Austria), the Sarntal Alps (Italy), the Dolomites (Italy), the Rocky Mountains (Colorado, USA) and on Spitsbergen (Svalbard, Norway). The second most abundant haplotype (H2) occurred on several sites in continental Norway and on Spitsbergen as well as in the Rocky Mountains (Colorado, USA). A smooth cell surface was typical for most of the haplotypes of red cysts, whereas pronounced nipples were found only in a single haplotype (H3) recorded from Italy and Svalbard. Small papillae were rare and only found in scattered cells in three specimens with smooth-walled cysts (Italy—'1D', Switzerland—'Furka', Slovakia—'Zamrznute') belonging to the most common haplotype (H1). *Sanguina aurantia* (small orange cysts) were represented here by two haplotypes (HA1 and HA2), reported from Svalbard and phylogenetically already attributed to a clade called 'Roter Schnee' (Leya 2004). The Austrian Alps were shown to be rich in haplotype diversity of *Sanguina nivaloides*, with the presence of at least five (H1, H4, H9, H10 and H13). The haplotype network of this species indicates the presence of shared haplotypes among European mountain ranges, between alpine and polar habitats (e.g. Austria versus Svalbard) and between the continents investigated (Europe, North America and South America). Interestingly, the small orange cysts of *Sanguina aurantia* were not restricted only to the island of Spitsbergen in Svalbard as was implied from preliminary conclusions, but its haplotypes HA2, HA3 and HA4 were found at sampling sites in Colorado and Washington (USA), as shown inSupplementary Fig. 7. The extended version of the haplotype network of *S. nivaloides* detected four further haplotypes for this species (sequence JP1 was phased into sequences belonging to H1 and H22, the latter was connected to the ITS2 haplotype network when the TCS connection limit was lowered to 91%), which confirmed its cosmopolitan distribution e.g. in Japan, Tajikistan, Greenland and Alaska. However, for these sequences published prior to this study, no scanning electron nor light microscopy pictures of cells were available for comparison.

Spatial structuring of *Sanguina nivaloides* metapopulations

The sPCA revealed positive and negative eigenvalues for both two *S. nivaloides* datasets, indicating global (positive values) and local (negative values) patterns. However, the tests on global and local structures were not significant ($P > 0.05$, Supplementary Table 10), so *S. nivaloides* showed an absence of a distinct global spatial genetic structure and no genetic differentiation between European regions (Supplementary Fig. 8). In other words, we did not find any phylogeographic signal in the distribution of *S. nivaloides*. Moreover, the Mantel test on pairwise geographic and genetic matrices showed no significant correlation (Supplementary Table 11). Genetic distances of *Sanguina nivaloides* ITS2 sequences within and between mountain ranges (European Alps, High Tatra Mountains, continental Norway, Rocky Mountains, Patagonia) and polar regions (Svalbard, Antarctica) were very similar (Table 2). These findings suggest a high dispersal capacity of the cysts, which could promote a continuous gene flow over long distances (on scales of different continents!). At the same time, a successful independent evolution of haplotypes in separate mountain ranges and polar regions might also be taking place as inferred from the genetic distances observed within these groups. That both scenarios are possible for *Sanguina nivaloides* is visualised by the geographical distribution of ITS2 haplotypes in its network (Fig. 9): an identical haplotype occurred in several regions, and a particular region was inhabited by a few different haplotypes.

Taxonomic treatment

***Sanguina* Leya, Procházková et Nedbalová, gen. nov.**

Type of the name of the genus: *Sanguina nivaloides* Procházková, Leya et Nedbalová, sp. nov.

Registration: http://phycobank.org/100627

Initially, we attempted to reinstate one of the old genus names typified by *Uredo nivalis* F.A.Bauer 1819—*Protococcus* C.Agardh, 1824 or *Sphaerella* Sommerfelt, 1824—but both genera names have to be rejected, in the former case versus *Chlamydomonas* Ehrenberg, 1833 (*nom. et orth. cons.*) (original publication: Ehrenberg 1834), in the latter versus *Chlorococcum* Meneghini 1842 (original publication: Meneghini 1843) (*nomen cons.*) (Farr and Zijlstra 1996+). The complicated historic synonymy and the fact that it is not possible to prove that *Uredo nivalis* F.A.Bauer 1819 is conspecific with our recent findings are the reasons why the newly established clade is described by us as a new genus and species.

Etymology: The genus name *Sanguina* refers to the striking blood-red colouration of snow caused by the bloom of its cysts.

Description: Cysts (it is unresolved whether these are of asexual or sexual origin) are spherical, contain one nucleus, a central chloroplast with one naked pyrenoid, and abundant peripheral lipid globules containing red-coloured carotenoids. According to the maturity of cysts and their astaxanthin to chlorophyll-*a* ratios, cysts can appear in different colour shades as orange-peel orange or blood red. As the secondary carotenoids are stored in lipid globules of different sizes the cytoplasm can appear speckled to homogeneous. The surface of the cysts can appear smooth, with blunt (nipples, papillae) or sharp (nibs) protrusions. In mature cysts, carotenoids mask other cell organelles beyond recognition. In young cysts a single parietal chloroplast is clearly visible. At the light microscopy level one cell wall layer can be distinguished in mature cysts and two layers in young cysts. The outermost layer in young cysts is most probably the primary cell wall, which later is shed during cyst maturation exposing the developing secondary cell wall. Vegetative stages are unknown, and no culturable strains exist.The genus is restricted in its habitat to snowfields and glacier-based snowfields in polar and alpine regions.

Diagnosis: The genus *Sanguina* differs from other genera within the Chlamydomonadaceae [i.e. the genus *Chlamydomonas* sensu Pröschold *et al.* (2001)] in its phylogeny, as this species

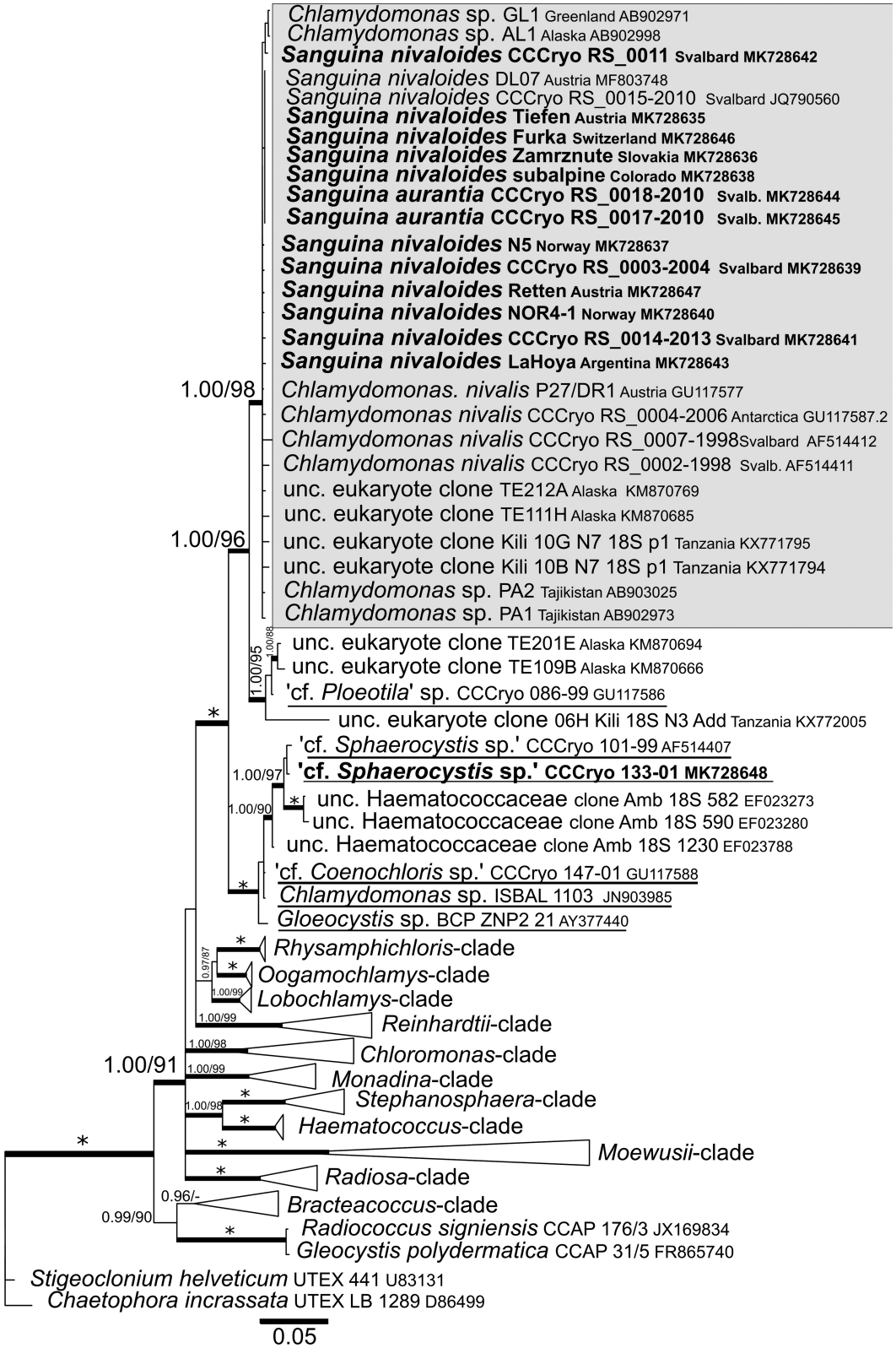

Figure 7. 18S ribosomal RNA gene-based Bayesian phylogenetic tree. The *Sanguina*-clade with *Sanguina nivalis* and *Sanguina aurantia* is highlighted in a grey box. Posterior probabilities (≥0.95) and bootstrap values from maximum likelihood analyses (≥75%) are shown. Full statistical support (1.00/100) is marked with an asterisk. Thick branches represent nodes receiving the highest posterior probability support (1.00). Newly obtained sequences are in bold. Accession numbers, strain or field sample codes are indicated after each species name. Species names of the closest species that are available as laboratory cultures are underlined. Abbreviation: unc, uncultured.

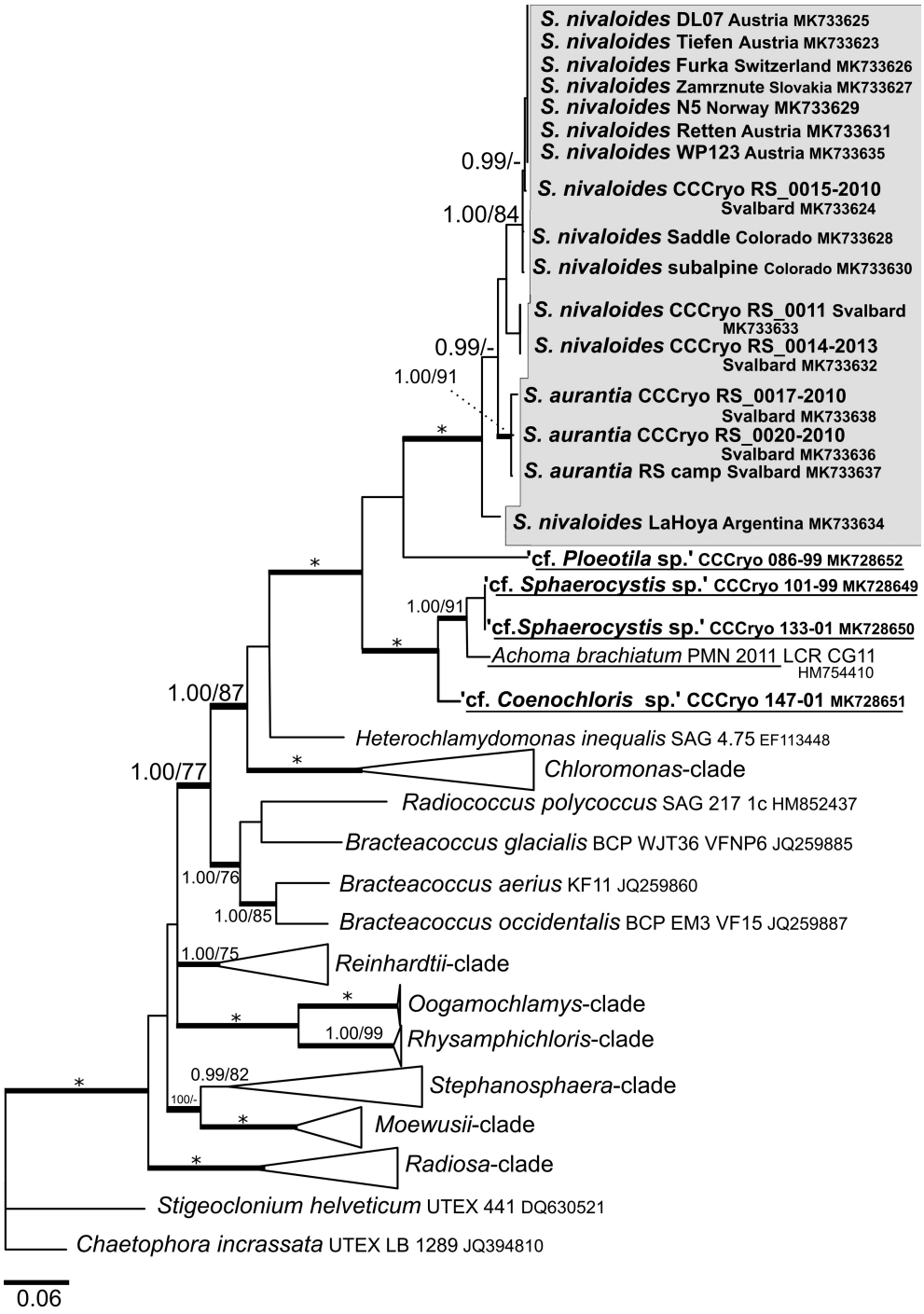

Figure 8. rbcL gene-based Bayesian phylogenetic tree. The *Sanguina* (*S.*)-clade with *Sanguina nivaloides* and *Sanguina aurantia* is marked in a grey box. Posterior probabilities (≥0.95) and bootstrap values from maximum likelihood analyses (≥75%) are shown. Full statistical support (1.00/100) is marked with an asterisk. Thick branches represent nodes receiving the highest posterior probability support (1.00). Newly obtained sequences are in bold. Accession numbers, strain or field sample codes are indicated after each species name. Species names of the closest species that are available as laboratory cultures are underlined.

forms an independent lineage in phylogenetic trees based on 18S rRNA gene (Fig. 7) or rbcL data (Fig. 8) [characteristic 18S rRNA gene and rbcL sequences for holotype specimen CCCryo RS 0015–2010: accession numbers JQ790560 (new resequencing of this field material in the course of this study resulted in the identical sequence) and MK733624, respectively]. Moreover, *Sanguina* is distinguishable from the genus *Chlamydomonas* in its clear habitat preference. The former genus develops cysts rich in astaxanthin, which causes the striking red or orange colouration of snow in alpine and polar regions. The morphology of vegetative stages of *Sanguina* is unknown because no culturable, proliferating strain exists, thus hampering a comparison of such life cycle stages to those of the genus *Chlamydomonas*. Regarding its fully spherical, red cysts, *Sanguina* differs from mature cysts of *Chlainomonas* sp. in its cell wall arrangement and plastid organisation: the latter has multilayered cell walls including an opaque

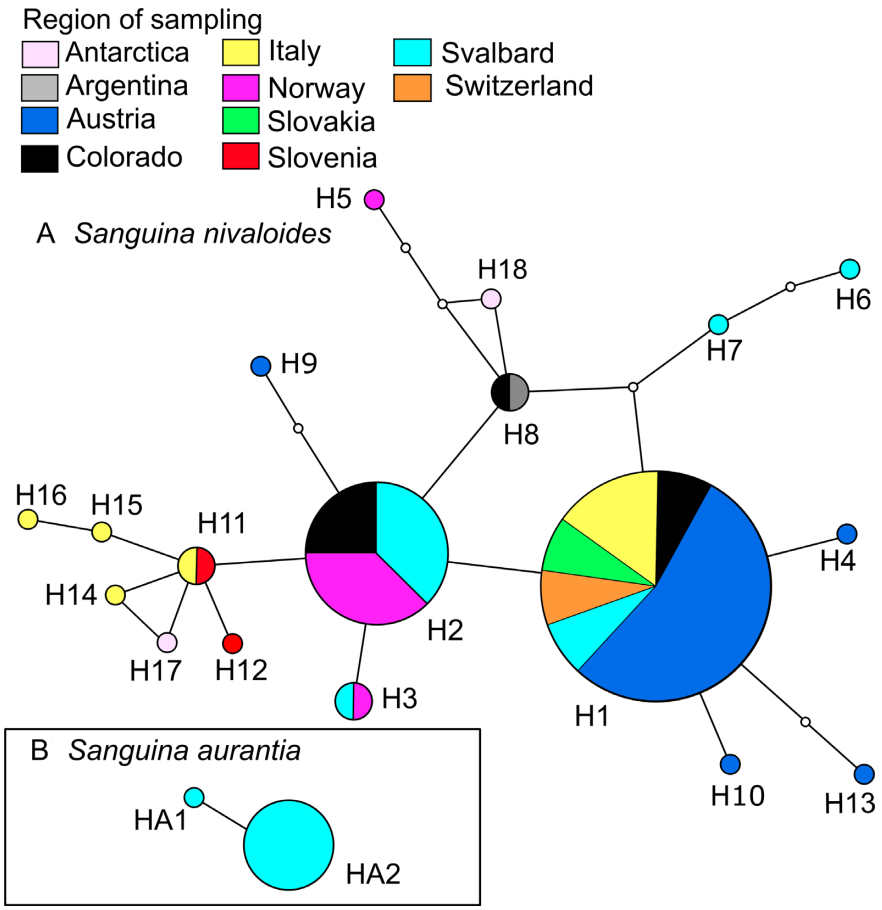

Figure 9. Geographic distribution of ITS2 rDNA haplotypes detected in this study: (**A**) *Sanguina nivaloides*, (**B**) *Sanguina aurantia*. Each haplotype network was constructed by a statistical parsimony method with a 95% connection limit. The *Sanguina nivaloides* network includes haplotypes from polar regions (Antarctica, Svalbard) and alpine regions in Europe (Austria, Italy, Norway, Slovakia, Slovenia, Switzerland), North America (Colorado) and South America (Argentina). The *Sanguina aurantia* network includes haplotypes from Svalbard. Each ball represents a haplotype (i.e. in this study's field samples, which have identical ITS2 sequences). The size of the ball is proportional to the number of specimens sampled, which belong to that specific haplotype. The colour represents a country of sampling. Lines connect each haplotype with its most similar relative. Open dots represent mutation steps between haplotypes, one dot indicates a change of one base pair.

Table 2. Mean uncorrected (p-distance; %) and corrected pairwise genetic distance (Kimura-2-parameter K2P; %) between *Sanguina nivaloides* field samples from different regions based on the ITS2 rDNA nucleotide sequence below and above the diagonal. Mean uncorrected and corrected pairwise genetic distances are shown in the first column. The presence of n.c. (not calculated) in the results denotes cases in which it was not possible to estimate evolutionary distances (single sequence from the region).

	Mean intraspecific distance	Svalbard	European Alps	Norway	Tatra Mountains	Rocky Mountains	Patagonia	Antarctica
Svalbard	1.30		1.20	1.20	0.80	0.90	1.00	1.60
European Alps	1.00	1.20		1.20	0.60	0.80	1.20	1.60
Norway	1.00	1.20	1.20		1.00	0.70	0.80	1.40
Tatra Mountains	n.c.	0.80	0.60	1.00		0.50	1.00	1.50
Rocky Mountains	0.50	0.90	0.80	0.70	0.50		0.50	1.10
Patagonia	n.c.	1.00	1.20	0.80	1.00	0.50		1.00
Antarctica	2.00	1.50	1.50	1.30	1.50	1.10	1.00	

layer, plastids are located close to the cell wall (parietal) and mean cyst sizes are larger in diameter (Procházková *et al.* 2018b). *Chlainomonas* sp. also differs in the blood-red, but ovoid quadriflagellate cell stages that are quite distinct from the immobile spherical cysts of *Sanguina*. Moreover, *Chlainomonas* sp. prefers water-logged habitats, and thus usually causes the red colouration of snow-slush on frozen lakes. *Sanguina*, on the other hand, is rather found in terrestrial habitats such as snow-covered rocks or soil and permafrost. If *Sanguina* is found close to water-logged localities, it tends to dwell on the dry parts of snow. *Smithsonimonas abbotii* (Kol 1942), a snow alga described from red snow above the timber line in Alaska, might be closely related to the genus *Chlainomonas*. It differs from *Sanguina* in its cells being surrounded by a bell-shaped cell wall, which is smooth when young and becomes progressively warty when older. Large quantities of astaxanthin are also accumulated in the resistant red cysts

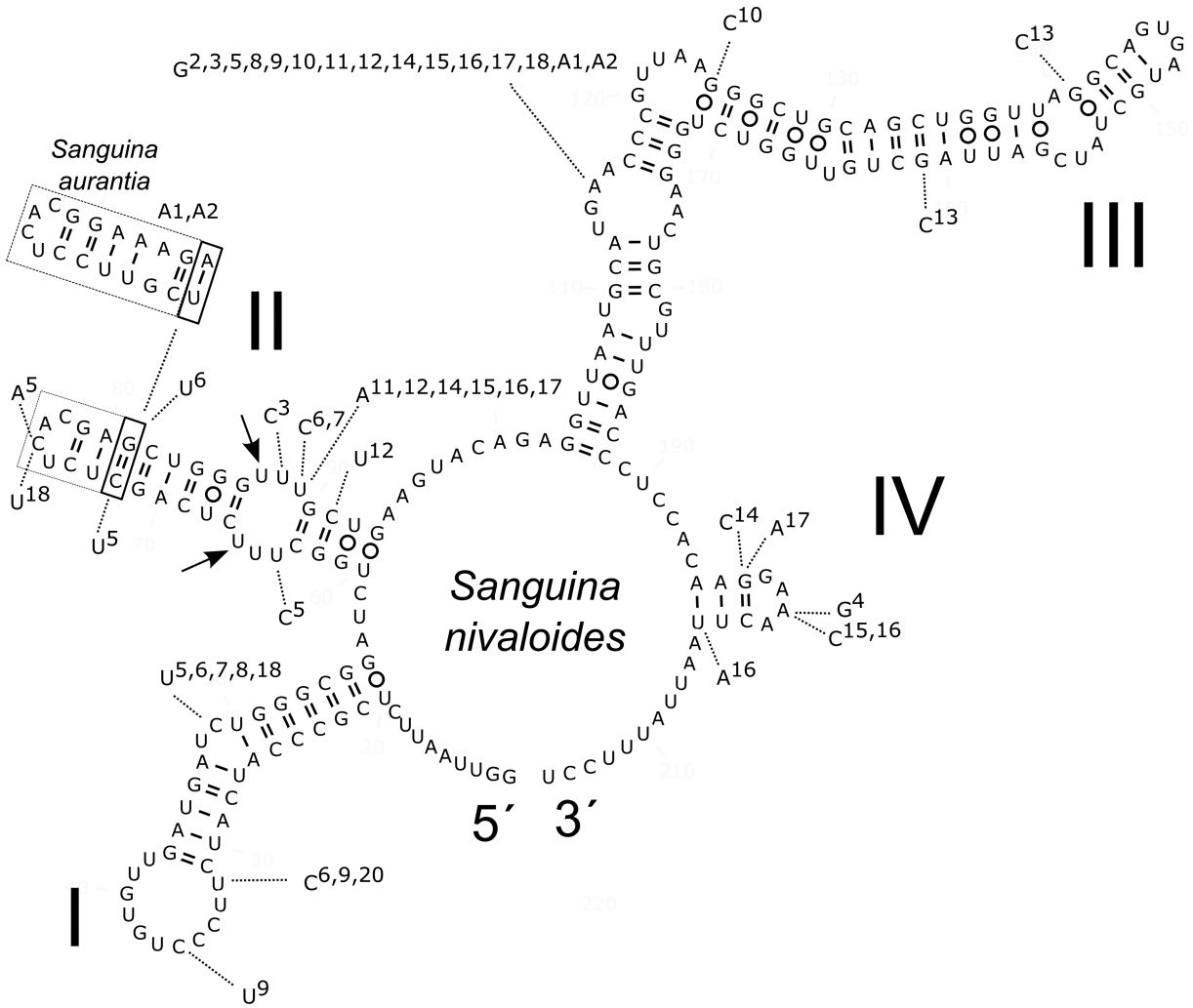

Figure 10. Comparison of the secondary structure of the ITS2 rDNA transcripts of 18 haplotypes of *Sanguina nivaloides* (H1-H18) and two haplotypes of *Sanguina aurantia* (HA1, HA2). Helices are labelled with Latin numbers (I-IV). Nucleotide differences of all haplotypes are shown outside the structure and are linked by dotted lines. Numbers 2–18, A1 and A2 indicate in which haplotype the difference was detected when compared to haplotype number 1 of *Sanguina nivaloides* (represented by the holotype specimen CCCryo RS_0015–2010, accession number MK728599). One compensatory base change between *Sanguina nivaloides* and *Sanguina aurantia* is indicated by the bold rectangle. The dashed rectangle at the end of helix II is showing an expansion segment (length is not conserved). Note: the U–U mismatch in helix II (arrows). The 5´ and 3´ ends of the ITS2 transcript are indicated.

(aplanospores) of the genus *Haematococcus* (Allewaert *et al.* 2015; Mazumdar *et al.* 2018), which differs, however, in its 18S rRNA gene and rbcL sequences.

***Sanguina nivaloides* Procházková, Leya et Nedbalová, sp. nov.**

? = *Uredo nivalis* F.A.Bauer, Microscopical observation on the red snow.— *The Quarterly Journal of Literature, Science and The Arts, London* : 222–229 (incl. plate VI), Figs 1-7. 1819

? = *Chlamydomonas nivalis* (F.A.Bauer) Wille, Algologische Notizen IX-XIV. Nyt Magazin for Naturvidenskaberne 41: 103, 126, plate III, Figs 44, 45. 1903.

Neither of the original field samples of *Uredo nivalis* from 1818 and of *Chlamydomonas nivalis* from Wille are traceable, therefore these names are included in the synonymy with a question mark.

Nomenclatural remarks: Though we clearly do not attempt to synonymise *Cd. nivalis* with *S. nivaloides*, simply because there is no conclusive way to do so, for completeness we want to give an overview of the nomenclatural complexity relating to *Cd. nivalis*. With regard to the type of material sampled in Baffin Bay in 1818, three homotypic synonyms are listed on the website of AlgaeBase (Guiry and Guiry 2018): *Uredo nivalis* F.A.Bauer 1819, *Protococcus nivalis* C.Agardh 1824 and *Sphaerella nivalis* (F.A.Bauer) Sommerfelt 1824. In this context *Uredo nivalis* represents the lectotype and basionym, still reflecting that the (colourless) globules were regarded as a fungus. The genus *Uredo* was typified by Persoon (1801) with its type species *U. betae* and thus is conserved against *Cd. nivalis*. Wrangel (1823) described *Lepraria kermesina*, the lectotype species of *Protococcus*, and he considered this lichen to be the organism causing the red snow. *L. kermesina* was then listed as a synonym of *Protococcus nivalis*. *Haematococcus* Flotow, 1844 was also listed as a synonym, but it was finally decided to exclude both, *Lepraria kermesina* and *Haematococcus*, from the synonymy (Andersen 2018). With regard to *Protococcus* C.Agardh, 1824 and *Sphaerella* Sommerfelt, 1824—both genus names have to be rejected, in the former case versus *Chlamydomonas* Ehrenberg, 1833 (original publication: Ehrenberg 1834) (*nom. et orth. cons.*), in the latter versus *Chlorococcum* Meneghini, 1842 (original publication: Meneghini 1843) (*nomen cons.*) (Farr and Zijlstra 1996+). In the Index Nominum Genericorum

and the literature, further synonyms for *Cd. nivalis* are listed. In her extensive and outstanding monography on the biology and limnology of snow and ice, Kol (1968) cites these synonyms, which are given here for completeness as well (some citations have been corrected, as far as possible, as wrong volume numbers or pages were cited originally): *Palmella nivalis* Hooker 1825, p. 184; *Coccochloris nivalis* Sprengel (ex parte) 1827, p. 373; *Coccophysium nivale* Link 1833, p. 342; *Gloiococcus grevillei* Shuttleworth 1840a, p. 54 and Shuttleworth 1840b, p. 405 resp.; *Discerаea nivalis* Vogt 1844, p. 217 with plate 1: Figs 1-5 (as '*Discerea nivalis*'); *Hysginum nivale* Perty 1852, p. 95; *Chlamydococcus nivalis* (F.A.Bauer) A.Braun nach F.Cohn 1861, p. 54, *Haematococcus nivalis* (F.A.Bauer) C.Agardh 1828-1835, Icon. Alg., *Haematococcus nivalis* Flotow 1844. Further information on the synonymy and references on world-wide findings of *Cd. nivalis* also can be found in Kol (1968).

Holotype: Specimen CCCryo RS_0015–2010 of field sample 004/10 consisting of cysts in a desiccated (non-viable) state in the herbarium of the Botanic Garden and Botanical Museum Berlin-Dahlem (herbarium acronym: B), Freie Universität Berlin, Königin-Luise-Straße 6–8, 14 195 Berlin, Germany, no. B 40 00 43192 [http://herbarium.bgbm.org/object/B400043192, represented by our Figs 2A and 3A.

Isotypes: (1) desiccated, under nitrogen, in the Micropalaeo Collection, Museum für Naturkunde, Leibniz Institute for Evolution and Biodiversity, Science, Invalidenstraße 43, 10 115 Berlin, Germany, no. ECO103, (2) frozen at -80°C at DNA-bank in the herbarium of the Botanic Garden and Botanical Museum Berlin-Dahlem (herbarium acronym: B), no. B GT 00 24094 [http://herbarium.bgbm.org/object/BGT0024094], (3) frozen at -150°C (in triplicate) in the SAG biobank at the Department Experimental Phycology and Culture Collection of Algae at the Goettingen University (EPSAG), Nikolausberger Weg 18, 37 073 Goettingen, Germany, nos. Z000696411, Z000696414, Z000696417, (4) frozen at -150°C (in triplicate) in the CCCryo biobank at the Fraunhofer Institute for Immunology & Cell Therapy, Branch Bioanalytics and Bioprocesses IZI-BB, Am Muehlenberg 13, 144 760 Postdam, Germany, nos. 2–07-02–14, 2–07-02–15, 2–07-02–16, and (5) desiccated (in triplicate) in the CCCryo biobank, nos. D2–07-02–17, D2–07-02–18, D2–07-02–19.

Type locality: a steep snowfield surrounded by moss vegetation and rocks, stretching down northwest to sea level from Mount Midterhuken (760 m a.s.l.), southwest of Mariasundet between Bellsund and Van Mijenfjorden, Nathorst Land, Svalbard, Norway (77°39'44.298"N 14°48'58.903"E; altitude: 15 m a.s.l., specimen CCCryo RS 0015–2010, collected on 4 August 2010 by Thomas Leya & Guntram Weithoff as collectors' sample number 004/10).

Paratypes: (1) Specimen CCCryo RS_0003–2004 frozen at -150°C in the CCCryo biobank at Fraunhofer IZI-BB, no. 2–07-02–21 (Figs 2E, 3B and 4F), (2) specimen WP123 frozen at -150°C in the CCCryo biobank at Fraunhofer IZI-BB, no. 2–07-02–22 (Figs 2B and 4C-E).

Paratype localities: CCCryo RS_0003–2004: northeastern part of Doktorbreen, Nathorst Land, Svalbard, Norway (77°34'0.001"N 16°53'59.999"E; altitude: 430 m a.s.l., collected on 6 August 2004 by Thomas Leya, sample number 013–01/04); WP123: Schwarzmoos, Kühtai, Stockach, Tyrol, Austria (47°13'35.0'N 11°01'03.1'E; altitude: 2352 m a.s.l., collected on 25 May 2017 by Lenka Procházková & Daniel Remias, sample number WP123).

Registration: http://phycobank.org/100628

Etymology: the species epithet refers to the habitat of this species (snow).

Description: Usually smooth-walled cysts (Figs 2A and 3A), which can also be ornamented more or less regularly with nipples (Figs 2E and 3B), blunt nibs, or small or pronounced papillae. Cysts of size 7.8–39 μm in diameter, causing red snow. The astaxanthin to chlorophyll-*a* ratio of the red cysts ranges between 20:1 and 34:1 depending on the level of cyst maturity (Bidigare *et al.* 1993; Müller *et al.* 1998; Remias, Lütz-Meindl and Lütz 2005). At the light microscopy level usually only one cell wall layer is distinguishable in mature cysts (Fig. 2A) (using TEM two layers are distinguishable, Fig. 4B) and two cell wall layers for young cysts in early stages of development (Fig. 2B) (using TEM three layers are visible, Fig. 4E). The detailed structure of the cell wall is usually visible in TEM only; it contains a very thin trilaminar sheath formed below the transient primary cell wall during morphogenesis of the secondary cell wall. In early cyst stages a parietal chloroplast is clearly visible in LM, as are a large unpigmented vacuole and a naked pyrenoid (Fig. 2B). The temporary third outermost cell wall in TEM is fuzzy (Fig. 4E). Vegetative stages are unknown, as no culturable strains exist. *Sanguina nivaloides* is an extremophilic alga living in melting snowfields in polar and alpine regions.

Diagnosis: In the stage of mature cysts *S. nivaloides* has a single chloroplast located in the central position surrounding one single nucleus; (nearly) its entire cytoplasm appears dark red due to the secondary carotenoid astaxanthin. It differs from aplanospores of the genus *Haematococcus*, which have their chloroplasts localised in the interspace between oil droplets, resulting in chloroplasts with a net-like appearance (Wayama *et al.* 2013). It differs from *Bracteacoccus engadinensis*, which also accumulates astaxanthin in its multinuclear coenoblasts, but only in the central area, and its chloroplast is also composed of several (4–10) polygonal discs (Ettl and Gärtner 2014). It differs from *Chlainomonas rubra*, *Chlainomonas kolii* and *Chlainomonas* sp. quadriflagellates in its spherical cell shape (the latter have an ovoid cell shape) and its cell wall organisation (in *C. rubra* the protoplast is surrounded by a massive sheath of gelatinous material, *C. kolii* has a net-like outer envelope, *C.* sp. has a partially thickened cell wall) and in the absence of flagellar grooves in their cysts; persistant flagellar grooves were observed in the thick-walled cysts for *C. kolii* and *C. rubra* at least during cyst formation (Hoham 1974; Novis *et al.* 2008). Most importantly, *S. nivaloides* differs genetically in its 18S rRNA gene and rbcL sequences from red aplanospores of the genus *Haematococcus* such as *Haematoccoccus lacustris* (epitype, strain SAG 34–1b; 18S: AF159369.1) (Hepperle *et al.* 1998; Nakada and Ota 2016) and *Haematococcus alpinus* (strain: LCR-CC-261f, 18S: MF093734, rbcL: MF093733) (Mazumdar *et al.* 2018). *Sanguina nivaloides* differs from *Sanguina aurantia* in the macroscopic coloration of snowfields (the latter causes orange snow), cell size ranges (the latter is usually smaller, up to 16 μm), pigmentation (the latter has one magnitude lower level of astaxanthin to chlorophyll–*a* ratio in mature cysts), distribution (the latter was found in the Arctic and subarctic regions in North America to date) and physical association between cells (*Sanguina nivaloides* has cells that are almost always solitary, whereas *Sanguina aurantia* is often clustered by means of mucilaginous sheaths surrounding the cells). The genus *Sanguina* forms a monophyletic clade, and *S. nivaloides* is unique in its ITS2 rDNA sequence. For the holotype specimen CCCryo RS 0015–2010 the ITS2 rDNA sequence is characteristic (accession number MK728599).

Distribution: melting snow in Europe, Asia, Africa, Antarctica, the Arctic, North America, South America, New Zealand and Australia.

***Sanguina aurantia* Leya, Procházková et Nedbalová, sp. nov.**

Holotype: specimen RS_0017–2010 of field sample 005/10–1b consisting of cysts in desiccated (non-viable) state in the herbarium of the Botanic Garden and Botanical Museum Berlin-Dahlem (herbarium acronym: B), Freie Universität Berlin, Königin-Luise-Straße 6–8, 14 195 Berlin, Germany, no. B 40 00 43197 [http://herbarium.bgbm.org/object/B400043197], represented by our Fig. 5B and D.

Isotype: frozen at -80°C at DNA-bank in the herbarium of the Botanic Garden and Botanical Museum Berlin-Dahlem (herbarium acronym: B), no. B GT 00 38001 [http://herbarium.bgbm.org/object/BGT0038001].

Type locality: snowfield at the south foot of Fugleberget, Isbjörnhamna, Hornsund, Wedel Jarlsberg Land, Svalbard, Norway (77°0'42.156"N 15°32'13.2"E; altitude: 55 m a.s.l., collected on 6 August 2010 by Thomas Leya & Guntram Weithoff, sample number 005/10–1b).

Registration: http://phycobank.org/101398

Etymology: the species epithet refers to the intracellular colouration of the mature cysts (orange).

Description: Usually smooth-walled cysts (Figs 5B), sometimes the outermost layer is wrinkled and when it is decomposed, the smooth cell wall below may appear. Cysts of size 6.2–15.5 μm, causing orange snow. The astaxanthin to chlorophyll ratio of the orange cysts ranges between 0.8:1 and 2.6:1 (Müller *et al.* 1998). At the light microscopy level usually only one cell wall layer is distinguishable in mature cysts (Fig. 5B) (using TEM two layers are distinguishable), in some cases also a distant cell wall layer is present (Fig. 5A; in TEM three layers are visible and the outermost third layer might be multilayered, Fig. 5E). The detailed structure of the cell wall is usually visible in TEM only; it contains a very thin trilaminar sheath formed below the transient primary cell wall during morphogenesis of the secondary cell wall. Vegetative stages are unknown, as no culturable strains exist.

Diagnosis: *Sanguina aurantia* differs from *Sanguina nivaloides* in the macroscopic orange colouration of snowfields (the latter causes red snow), cell size ranges (the latter is usually larger, up to 40 μm), pigmentation (the latter has a higher level of astaxanthin to chlorophyll-*a* ratio in mature cysts), distribution (the latter was shown to be cosmopolitan) and physical association between cells (*Sanguina aurantia* is often clustered by means of a mucilaginous sheath surrounding the cells, whereas *Sanguina nivaloides* has cells that are almost always solitary). For the holotype specimen CCCryo RS_0017–2010 the ITS2 rDNA sequence is characteristic (accession number MK728634).

Distribution: in melting snow in subpolar and polar regions, so far the known locations are only in the northern hemisphere (North America, the Arctic).

DISCUSSION

The first collections of red snow date back to British expeditions to the far north looking for a navigable North-West passage (N.N. 1818; Bauer 1819; Ross 1819; Bauer 1820; Ross 1820). In our study many samples of red snow cysts from around the world have yielded sequences that fell in the new clade *Sanguina*, so one is tempted to assume that the historical sample of 1818 also probably represents the red snow-causing species *S. nivaloides*; however, this cannot be proven yet. A genetic comparison was not possible as the historic sample of 1818 could not be located in museums or herbaria in either London or Berlin. Intact DNA could also not be isolated from the similar sample collected during the Grinnell Arctic Expedition at Beverly Greenland [76°3' N in 1851 (Ehrenberg 1851; Leya 2008) a bit further north of the original location of 1818–1819 at the Crimson Cliffs (75°54' North, 67°15' West)]. Thus, we do not attempt to synonymise *S. nivaloides* with *Cd. nivalis*. In this study we have suggested that all our investigated red and orange spherical cysts belong to *Sanguina nivaloides* and *Sanguina aurantia*, respectively. We showed that the genus *Sanguina* forms one independent lineage in the Chlamydomonadaceae. The conservative nuclear marker 18S was 100% identical for these two species. Strains CCCryo 086–99, CCCryo 101–99, 133–01 and 147–01 represent the most closely related and culturable isolates/species and appear to be distributed into several lineages that are sister genera to the clade of *Sanguina*, some of them possibly representing the genus *Achoma* (Novis and Visnovsky 2012). The revised genus *Chloromonas* (Pröschold *et al.* 2001) so far contains the majority of other culturable snow algal species involved in coloured snow, but is robustly separated from the *Sanguina*-clade.

This study is the first record of ITS2 sequence data of spherical cysts forming red snow from Argentina and many mid-latitude alpine sites in Europe. Moreover, our data will increase the knowledge about this taxon due to several new findings on Svalbard. The ITS2 marker was previously used in this context only in studies of snow samples from the USA (Brown, Ungerer and Jumpponen 2016), Greenland, Alaska, Japan and Tajikistan (referenced in accession numbers only, see Materials and Methods) and also most recently from Antarctica and Svalbard (Segawa *et al.* 2018). The set of different molecular data used in this study has proved to provide valuable insights into the relationship of this taxonomically complex algal group. Haplotype networks have been used to demonstrate the intraspecific diversity (i.e. within a species) (Škaloud *et al.* 2015). Based on our results, *S. nivaloides* represents a diverse species containing 18 different ITS2 genotypes and *S. aurantia* has two ITS2 genotypes. According to the metagenomic study of Brown, Ungerer and Jumpponen (2016) in Colorado and Washington (USA), sequences of this locus of cysts in blooming snowfields were distributed into 30 haplotypes classified as '*Coenochloris*' and 27 haplotypes termed as '*Chlamydomonas*'. Further samplings in other mountain regions might reveal additional unique genotypes as shown by Segawa *et al.* (2018). Similarly, 15 haplotypes of ITS2 rDNA were resolved for the common 'blood rain alga' *Haematococcus lacustris* (referred to as *H. pluvialis* in the paper cited) in temperate Europe (Allewaert *et al.* 2015). Intraspecific diversity within the widespread lichen photobiont *Asterochloris lobophora* in Europe, America and Asia accounted for 18 haplotypes of ITS2 rDNA, while half that amount of intraspecific diversity was found for other *Asterochloris* species (Škaloud *et al.* 2015).

Although the overall mean distance among the ITS2 red cysts haplotypes of *S. nivaloides* was rather low [p-distance of 1.7%; this value was similarly low for *Asterochloris* lineages described by Škaloud *et al.* (2015)], a divergence between haplotypes can be observed with regard to the red cysts of *Sanguina nivaloides* and orange cysts of *S. aurantia* in their variable ITS2 marker (sequence differences up to 5%), which might indicate a currently ongoing genetic diversification. Such a process was described for the soil alga *Bracteacoccus bullatus* by Fučíková and Lewis (2012). Further detailed pigment studies, physiological experiments with cysts, sequencing of further highly variable molecular markers (Škaloud *et al.* 2015) and cultivation attempts, possibly using strategies so far unconsidered, are clearly necessary to bring a richer understanding of morphological and molecular variability within the genus *Sanguina*.

When comparing red snow samples of Baffin Bay (Greenland) from 1851 with our recent samples, this showed that cell sizes corresponded well to the cell size ranges determined in this study (Fig. 6). Spherical red globules as well as green globules 'mostly with a small stalk and fluffy attachment, being the thallus or the root and leaf layer' were reported from this sample [quotation translated into English from Ehrenberg (1851)]. While we could identify the former in the desiccated sample, the latter were not visible. However, we have also occasionally observed such stalks in recent samples [Fig. 2b in Leya (2008)]. We assume that they are fungal mycelia, which are not rare in field samples of red snow (Brown, Olson and Jumpponen 2015).

Cysts of *Sanguina nivaloides* are usually smooth-walled, and other specific variations in cell surface structure (e.g. cysts with nipples) may either reflect a level in the process of cyst maturation reached at the time of sampling or a causality between intraspecific variability and morphology (as e.g. all samples of H3 are expected to be represented by cysts with nipples, which is the case for both specimens of H3 in this study). To test this hypothesis, more specimens of the same morphologically different haplotype are needed (i.e. for H7, H14). Additionally, the observation of populations of smooth-walled cysts with the rare presence of cells with small papillae in two of our samples is in good correspondence with the findings reported from red snow in North America by Brown, Ungerer and Jumpponen (2016): they point out that very low haplotype diversity exists within the same algal bloom sampled: each algal patch was dominated by only one haplotype, with a very minor proportion of subdominant haplotypes. In the past, blooms of other snow algal taxa producing red cysts were often wrongly assigned to '*Chlamydomonas nivalis*', e.g. most often *Chlainomonas* was not recognised [see Figs 23 and 24 in Stein and Amundsen (1967), in Kawecka (1981), and in Fig. 4 in Kobayashi and Fukushima (1952)]. The first comprehensive cell ultrastructure and secondary pigment profile comparisons between cysts of *Chlainomonas* and '*Chlamydomonas nivalis*' were performed by Remias *et al.* (2016).

In our study, cell sizes of *S. nivaloides* red cysts correspond to the findings of Mosser *et al.* (1977) and Remias *et al.* (2005). The sizes of *S. aurantia* orange-coloured cysts from our study are in the range reported from Arctic pack ice floes (Gradinger and Nürnberg 1996) and from Spitsbergen (Müller *et al.* 1998; Leya 2004; Stibal *et al.* 2007). We assume that cell size can be highly plastic during their seasonal development, which would also explain the variable cell sizes among the haplotypes of red cysts we found, since our locations were sampled at different times during the snow melting season and were also varying in aspects related to their topographical properties (snowfield's slope angle, cardinal orientation of the site to the sun, elevation) and snow texture. Interestingly, the largest mean cell sizes were observed in samples collected either late in the season (e.g. samples '2RON', 'NOR4–1') or on glacier-based snowfields (e.g. samples '4HT', 'Foxfona', 'Retten'). Indeed, cell sizes may also reflect culture conditions as in the lichen photobiont *Asteriochloris* (Škaloud *et al.* 2015). An alternative hypothesis could be that cell sizes of *S. nivaloides* and *S. aurantia* haplotypes are genetically determined with some variability. Interestingly, we observed narrow cell size variations when comparing genetically very uniform small orange cysts of *S. aurantia* from the different locations on Svalbard (two haplotypes only). More observations of orange cysts of *S. aurantia* from other geographic regions are needed to test this hypothesis, e.g. a bloom in North America was genetically identical for ITS2 (accession number KX063716; Brown, Ungerer and Jumpponen 2016) to *S. aurantia* orange cysts sampled in Svalbard (this study), but for the former no morphology data were collected. Interestingly, some haplotypes of *S. nivaloides* red cysts [i.e. H9 ('WP123'), H18 ('Esperanza-8')] were as small as *S. aurantia* orange cysts. Considering this fact, the sole parameter of cell size only should not be used for distinguishing between *S. nivaloides* and *S. aurantia* by light microscopy. Other aspects of mature cysts also should be considered such as cell wall morphology, intracellular pigmentation reflecting the astaxanthin to chlorophyll-*a* ratio and the macroscopic colour of the blooming snowfield.

Due to their small size (Wilkinson *et al.* 2012) and ability to resist drought and freezing stress, the cysts of *S. nivaloides* and *S. aurantia* are suitable propagules for long distance dispersal by prevailing air streams (Brown, Larson and Bold 1964; Schlichting Jr. 1969), birds (e.g. polar birds migrating between the two polar regions, such as the Arctic tern *Sterna paradisaea*) and ocean currents (Gillespie *et al.* 2012). Our data showed a cosmopolitan distribution of *S. nivaloides* in alpine and polar snowfields in both hemispheres, which supports the theory of a trans-equatorial dispersal of microbes (Hodač *et al.* 2016). No population structure was detected when analysing the ITS2 rDNA data, as there was no phylogeographic signal. Metagenomic analyses have shown red pigmented snow algae to be cosmopolitans based on the analysis of partial sequences of the 18S rRNA gene (Lutz *et al.* 2016) as well as of the ITS2 rDNA (Segawa *et al.* 2018). The latter study also detected endemic snow algal phylotypes being distributed in one of the two polar regions. Antarctica was regarded for a long time as a continent in biological isolation until large amounts of vascular plant pollen were collected on Signy Island (South Orkney Islands), and a parallel observation of the daily synoptic weather patterns revealed that roughly 1.5 times per year a corridor of strong winds develops between Tierra del Fuego (Argentina) and Antarctica (Marshall 1996). This explains our finding that the South American sample of *S. nivaloides* ('La Hoya', H8) was nearly identical in its ITS2 rDNA sequence with the haplotype from maritime Antarctica (H18) and with the most common haplotype in Europe (H1). The distribution of these small microorganisms could be controlled by selection due to local environmental factors as well as dispersal limitations. Moreover, a strong founder effect from only few propagules and intense kin competition is assumed to take place (Brown, Ungerer and Jumpponen 2016).

Concerning local environmental factors at the moment of sampling of encysted cells, the usually slightly acidic pH and low conductivity of snow patches with algal blooms resembled those of pristine, white snow presumably free of any algae. However, Brown and Jumpponen (2019) showed that snow algae are seemingly omnipresent, though in low abundances, at the surface of melting subpolar and alpine 'white snow' that are void of a visible algal bloom. Nitrate, ammonium and phosphate were not limiting nutrients for Arctic algal communities in a study by Spijkerman *et al.* (2012). On the other hand, atmospheric trace gases were recently recognised to play a role in supporting primary production in oligotrophic habitats in polar regions (Ji *et al.* 2017). None of these findings conclusively explains the patchy occurrence of red snow, which often can be observed in the same pattern year after year at the same location. Spijkerman *et al.* (2012) suggested that the highly patchy distribution of algal blooms in snow could be partly a result of small-scale topographical and geological characteristics influencing snowfield persistence or disappearance due to enhanced or reduced snow melt or snow accumulation. Similarly, inputs of mineral impurities can result in significantly earlier snow melt (Di Mauro *et al.* 2018). The slower the melting, the more prolonged is the period that is available for a snow algal population to develop. This is realised

in alpine regions at higher elevations (above 1900 m a.s.l. in this study). With regards to the availability of liquid water, the algal cells seem to thrive during the growth season in the thin but persistent aqueous reservoir that by the laws of physics remains liquid around and between snow and ice crystals (Jones *et al.* 2001). To find a conclusive answer about which factors on a small scale actually determine the development of snow blooms such as those of *S. nivaloides* and *S. aurantia* or whether the cysts are just randomly dispersed there, a time series sampling would be necessary to observe the development of a blooming snow field while concurrently measuring various parameters.

Red spherical cysts from the European Alps morphologically identical to *S. nivaloides* cysts were shown to tolerate short periods of elevated UV-B radiation (Remias *et al.* 2010) due to the massive production of secondary carotenoids, which act mainly as shading pigments, but also as very powerful radical scavengers. This is especially true of ketocarotenoid astaxanthin, which absorbs energy in the near UV-range. *Sanguina nivaloides* shows high photophysiological plasticity with a highly efficient photosystem under low irradiation and no photoinhibition up to 2000 μmol m^{-2} s^{-1} (Procházková *et al.* 2018b). Additionally, inorganic rock dust particles covering mature cysts seem to provide additional shading protection (Lutz-Meindl and Lutz 2006). *Sanguina nivaloides* cysts are required to survive over summer when snow has melted, and provided they still contain chlorophyll and are not photoinhibited, the photosynthetic apparatus should continue to function (Remias, Lütz-Meindl and Lütz 2005). After total snow melt, cysts most likely 'oversummer' the rest of the year, generally in a dried state, on rocks, permafrost or moss-covered soil, all being subject to drastic diurnal temperature fluctuations; non-vegetated soils in particular can experience temperature changes of 30°C within 24 h (Ley, Williams and Schmidt 2004). Therefore, *S. nivaloides* cysts can be regarded as being eurythermic and desiccation-resistant. The question remains whether the vegetative stages (gametes or other green stages if they exist) are dependent on cold temperatures, which would characterise them as cryophiles.

Key triggers to a successful *S. nivaloides* cultivation have not been elucidated yet. Indeed, many green proliferating strains have been isolated from snowfields, but molecular methods and phylogeny have always shown that these isolates are taxa other than *S. nivaloides*. A well-known example of such a misinterpretation was strain UTEX 1969, which for years was listed as *Chlamydomonas nivalis* and frequently used in studies addressing cold adaptation, just as other strains erroneously were assigned to this taxon (Lu *et al.* 2012a,b, 2016). When, in 1990, H. Ettl and U.G. Schlösser (pers. comm.) re-identified many UTEX, CCAP and SAG strains of *Chlamydomonas*, they found that many were incorrectly named—among them also *Cd. nivalis* strains, which were first assigned to *Chlamydomonas augustae*, but later partly renamed again on the basis of the phylogenetic analyses as *Chloromonas typhlos* (Matsuzaki, Hara and Nozaki 2012) or *Cr. reticulata* (CCALA 753; CCALA 754). At present, it must be accepted that we do not have any living strain on hand to enable the studies on the life cycle of *S. nivaloides*. All diagrams describing the life cycle of this species are thus just hypothetical without any empirical proof (e.g. in terms of molecular data) (Müller, Leya and Fuhr 2001; Sattler *et al.* 2010; Remias 2012). Any conclusions can be made only very cautiously and indirectly based on the knowledge of life cycles of more distantly related species. The sexual life cycle of several Chlamydomonadacean species usually include the formation of zygotes into zygospores with a thick cell wall, which represents the dormant stage in the life cycle (Žárský, Kalina and Sulek 1985). After the formation and growth of the secondary cell wall, the primary cell wall of the zygospore is shed from the surface (VanWinkle-Swift and Rickoll 2008) and the ornamented structure of the mature zygote becomes apparent (Pröschold *et al.* 2001). We observed a similar cell wall organisation in the ruby cysts type, which have been found so far on the Northern hemisphere in continental Norway (sample N4' and NOR4–1' in this study), in Svalbard [sample RS_0011 in this study and in Müller *et al.* (1998)], on Iceland (D. Remias, pers. comm.), on the western coast of Canada (L. Quarmby, pers. comm.), in Washington State in the USA (K. Thomas, pers. comm.), Oceania (P. Novis, pers. comm.), as well as in the southern hemisphere on the Antarctic King George Island (T. Leya, pers. comm.). Wille (1903) was referring to this distinctive cellular morphology in his study of *Cd. nivalis* from Djupvatshytten (Norway) (plate III, Figs 44 and 45). Their identity needs to be revealed by single cell sequencing. The first insights into their 18S rRNA gene phylogeny suggest that the ruby-type cysts might in fact be members of the *Chloromonas*-clade (Segawa *et al.* 2018).

The CBC species concept was successfully applied for several algal groups, e.g. snow-dwelling *Chloromonas* species (Matsuzaki *et al.* 2019). This concept can be used also in a metagenomic study: Segawa *et al.* (2018) showed that their '*Chlamydomonas*' snow group B (conspecific with *S. nivaloides*) differs by one CBC in helix III only compared with the closely related '*Chlamydomonas*' snow group A (see their Supplementary Figures S2 and S8). On the other hand, it was shown that the CBCs are not diagnostic in some cases at the species level and that even genera, families and orders of green algae can lack CBCs in such regions (Caisova, Marin and Melkonian 2011; Škaloud and Rindi 2013). Therefore, the presence and number of CBCs are probably direct consequences of the accumulation of mutations during the evolutionary process, simply reflecting the genetic distance among organisms. In our study, two field samples of *Sanguina nivaloides* ('NOR4–1' and 'RS_0014–2013') lack any CBC in their secondary structure when compared with *Sanguina aurantia*. Both two newly described species are closely related: they have identical 18S rRNA gene and more than 95% identical ITS2 (one CBC found). In the rbcL phylogeny, *S. aurantia* has been placed within *Sanguina nivaloides* field samples; this might be linked to unusual gene substitutions in rbcL, which was reported to result in artefacts in the phylogeny (Nozaki, Onishi and Morita 2002). Species boundaries between *S. nivaloides, S. aurantia* and other related species should be estimated by combination of substantial morphological, ecological and genetic difference (investigation of several molecular markers, the level of ITS2 rDNA sequence similarity should be also taken into account). *S. aurantia* has uniquely different ITS2 haplotypes to *S. nivaloides*, orange spherical cysts and red spherical cysts are clearly distinguishable, both microscopically and macroscopically, and the area of their geographic distribution is only partly overlapping. No strain for these species is available yet. According to our 18S rRNA gene and rbcL phylogenies, the closest known and culturable relatives of *Sanguina nivaloides* are strains CCCryo 133–01/101–99 (currently assigned to cf. *Sphaerocystis* sp.), strain CCCryo 147–01 (cf. *Coenochloris* sp.) and CCCryo 086a-99 (cf. *Ploeotila* sp.). Some of these relatives are known for their production of astaxanthin (Leya *et al.* 2009), though in less dominating amounts than in *S. nivaloides*, but none of them has ever been reported to cause striking snow colouring. They have been isolated from different habitats on Svalbard such as a moss and a snowfield as well as from a glacier. These strains may rather be regarded as permafrost algae than snow algae. Demchenko (2013) investigated the above strains and described them all as having coccoid cells.

When studying their life cycles he observed zooid formation in strains CCCryo 101–99 and CCCryo 086b-99. Motile stages so far have not been described for the only known species of *Ploeotila* (*P. ramosa* T.Mrozinska-Webb) and since he also found slightly different characteristics in the other two strains in comparison to *Sphaerocystis* or *Coenochloris*, their attribution to these genera remains unclear (hence the 'cf.'). Our rbcL phylogeny (Fig. 7) confirmed that these tentative genera form closely related lineages to *Achoma brachiatum* isolated from an alpine herbfield soil in New Zealand (Novis and Visnovsky 2012). However, as outlined above, CCCryo 101–99 and 133–01 clearly differ from strain CCCryo 147–01, the former two producing zoids and considerable amounts of secondary carotenoids and the latter lacking such cell stages and ability. Which of them actually might have to be assigned to the genus *Achoma* remains to be investigated. The three strains CCCryo 086a-99, 101–99 and 147–01 further markedly differ in the following aspects: cells are single or organised in clusters of tetrads in CCCryo 133–01, in microscopic colonies in an extracellular polymeric substance (EPS) in CCCryo 147–01, and in cells or a group of cells sitting on a mucilaginous stalk in CCCryo 086a-99. Chloroplasts are parietal (CCCryo 133–01, CCCryo 086a-99) and pot-like (CCCryo 147–01), and a pyrenoid is present. Yet *S. nivaloides* shares several features with the above mentioned three CCCryo strains: its origin from cold habitats, its parietal chloroplast with a pyrenoid (at least observable in young cysts) and its prevailing morphologic organisation as a coccoid life form.

Our study has shown that sequencing of the field-collected cysts was a suitable strategy and also the only option to decipher their phylogenetic position, as establishing actively growing isolates from them has yet to be successful. This newly described genus *Sanguina* with two closely related species *S. nivaloides* and *S. aurantia* represents a single monophyletic lineage, independent from other Chlamydomonadacean algae. Using molecular methods we showed that *S. nivaloides* has a cosmopolitan distribution in polar and alpine regions, having detected the same ITS2 haplotypes on several continents. It is possible to distinguish the cysts of *S. nivaloides* from red-coloured cysts of other algae based on the cell size, number of cell walls, plastid organisation and habitat preference. Further studies could involve single-cell sequencing methods, e.g. with a further focus on the ruby-type cysts. The genetic variability below species level might be detected using a microsatellite-based approach (Nagai *et al.* 2007) developed from single cell genomics (Muramoto *et al.* 2010). Additionally, sampling at known locations early in the season might help to discover vegetative stages of this species, enabling us to study this interesting alga in much more detail using viable cultures/isolates. The molecular identity of other red coccoid species from snow reported by Kol (1968) such as *Chlamydomonas antarcticus* (red cysts with a broad mucilage layer) or *Trochiscia* spp. (red cysts with spikes) might also yet be revealed.

SUPPLEMENTARY DATA

Supplementary data are available at FEMSEC Journal online.

ACKNOWLEDGEMENTS

We thank Petr Sklenář, Marie Bulínová, Adéla Moravcová, Eva Hejduková, Martin Pusztai (all: Charles University, Prague, Czech Republic) and Daniel Remias (University of Applied Sciences Upper Austria, Wells, Austria) for field sampling. Our sincere thanks to Jasna Vukić (Charles University, Prague, Czech Republic) for her hints concerning haplotype network reconstruction. We are immensely grateful to Wolf-Henning Kusber (Botanischer Garten und Botanisches Museum Berlin, Germany) for his comments and great help with the taxonomic treatment. We also thank David Lazarus (Museum für Naturkunde, Berlin, Germany) for letting us have some of the historical red snow field sample of 1851. TL is specifically thankful to Günter R. Fuhr for having made numerous scientific voyages to Svalbard and the Antarctic and many invaluable experiences in the Arctic possible. We thank the reviewers, explicitly Phil Novis, for their constructive comments.

FUNDING

This work was supported by the Czech Science Foundation (GACR) project [18–02634S to LP and LN] and by the institutional long-term research plan RVO67985939 of the Institute of Botany of the Czech Academy of Sciences.

Conflicts of interest. None declared.

REFERENCES

Agardh CA. Systema Algarum. *Lundae* 1824;**XI-XXI**:13–4.

Agardh CA. *Icones Algarum Europaerum*. Leipzig: Leopold Voss, 1828–35.

anagreh L, Pegg C, Harikumar A *et al.* Assessing intragenomic variation of the internal transcribed spacer two: Adapting the Illumina metagenomics protocol. *PLoS One* 2017;**12**:e0181491.

Allewaert CC, Vanormelingen P, Pröschold T *et al.* Species diversity in European *Haematococcus pluvialis* (Chlorophyceae, Volvocales). *Phycologia* 2015;**54**:583–98.

Andersen RA. Report of the nomenclature committee for algae: 19. *Taxon* 2018;**67**:1029–30.

Bauer F. Microscopical observation on the red snow. *Quart J Sci Arts* 1819;**7**:222–9(incl. plate VI).

Bauer F. Red snow of Baffin's Bay. *Amer J Sci Arts* 1820;**2**:356.

Bidigare RR, Ondrusek ME, Kennicutt MC, II *et al.* Evidence for a photoprotective function for secondary carotenoids of snow algae. *J Phycol* 1993;**29**:427–34.

Brown RM, Larson DA, Bold HC. Airborne algae: Their abundance and heterogenity. *Science* 1964;**143**:583–4.

Brown SP, Jumpponen A. Microbial ecology of snow reveals taxa-specific biogeographical structure. *Microb Ecol* 2019;**77**:946–58.

Brown SP, Olson BJSC, Jumpponen A. Fungi and algae co-occur in snow: An issue of shared habitat or algal facilitation of heterotrophs? *Arctic, Antarctic, and Alpine Research* 2015;**47**:729–49.

Brown SP, Ungerer MC, Jumpponen A. A community of clones: Snow algae are diverse communities of spatially structured clones. *Int J Plant Sci* 2016;**177**:432–9.

Caisová L, Marin B, Melkonian M. A close-up view on ITS2 evolution and speciation - a case study in the Ulvophyceae (Chlorophyta, Viridiplantae). *BMC Evol Biol* 2011;**11**:262.

Caisová L, Marin B, Melkonian M. A consensus secondary structure of ITS2 in the Chlorophyta identified by phylogenetic reconstruction. *Protist* 2013;**164**:482–96.

Clement M, Posada D, Crandall K. TCS: A computer program to estimate gene genealogies. *Mol Ecol* 2000;**9**:1657–9.

Cohn F, *Chlamydococcus nivalis* (F.A.Bauer) A. Braun. *Rabenhorst: Algae Exsiccatae*., 1861, **1141**.

Coleman AW. The significance of a coincidence between evolutionary landmarks found in mating affinity and a DNA sequence. *Protist* 2000;**151**:1–9.

Coleman AW. Pan-eukaryote ITS2 homologies revealed by RNA secondary structure. *Nucleic Acids Res* 2007;**35**:3322–9.

Czygan F-C. Blutregen und Blutschnee: Stickstoffmangel-Zellen von *Haematococcus pluvialis* und *Chlamydomonas nivalis*. *Arch Mikrobiol* 1970;**74**:69–76.

Darty K, Denise A, Ponty Y. VARNA: Interactive drawing and editing of the RNA secondary structure. *Bioinformatics* 2009;**25**:1974–5.

Demchenko E. Morphology, ecophysiology and molecular phylogeny of marine and psychrophilic green flagellates belonging to *Microglena* and their adaptation to changing ecological conditions. *DAAD Reports*. 2013;**322**:1–15.

Demchenko E, Mikhailyuk T, Coleman AW *et al*. Generic and species concepts in *Microglena* (previously the *Chlamydomonas monadina* group) revised using an integrative approach. *Eur J Phycol* 2012;**47**:264–90.

Di Mauro B, Garzonio R, Rossini M *et al*. Saharan dust events in the European Alps: Role in snowmelt and geochemical characterization. *The Cryosphere* 2019; **13**:1147-65.

Ehrenberg CG. Dritter Beitrag zur Erkenntnis großer Organisation in der Richtung des kleinsten Raumes. *Physikalische Abhandlungen der Koeniglichen Akademie der Wissenschaften zu Berlin* 1834;**1833**:145–336.

Ehrenberg CG, König. Preuss. Akad. Wiss. Berlin. Über eine frische Probe der die Crimson Cliffs scharlachroth färbenden Substanz aus der Baffins Bai und das sie begleitende kleinste Leben. Bericht über die zur Bekanntmachung geeigneten Verhandl. 1851:741–4.

Ettl H, Gärtner G. *Syllabus der Boden-, Luft- und Flechtenalgen*. Springer, 2014.

Farr ER, Zijlstra G. Index nominum genericorum (Plantarum), 1996+. http://botany.si.edu/ing/ (18 March 2019, date last accessed).

Fjerdingstad E, Kemp K, Fjerdingstad E *et al*. Chemical analyses of red "snow" from East-Greenland with remarks on *Chlamydomonas nivalis* (Bau.) Wille. *Arch Hydrobiol* 1974;**73**:70–83.

Flotow J. Über *Haematococcus pluvialis*. *Nov Act Leop Carol* 1844;**20**:413–606.

Fučíková K, Lewis LA. Intersection of *Chlorella*, *Muriella* and *Bracteacoccus*: Resurrecting the genus *Chromochloris* Kol et Chodat (Chlorophyceae, Chlorophyta). *Fottea* 2012;**12**:83–93.

Gillespie RG, Baldwin BG, Waters JM *et al*. Long-distance dispersal: A framework for hypothesis testing. *Trends Ecol Evol* 2012;**27**:47–56.

Gradinger R, Nürnberg D. Snow algal communities on arctic pack ice floes dominated by *Chlamydomonas nivalis* (Bauer) Wille. *Proc NIPR Symp Polar Biol* 1996;**9**:35–43.

Guiry MD, Guiry GM. AlgaeBase. World-wide electronic publication, National University of Ireland, Galway, 2018. http://www.algaebase.org (14 June 2018, date last accessed).

Hepperle D, Nozaki H, Hohenberger S *et al*. Phylogenetic position of the Phacotaceae within the Chlamydophyceae as revealed by analysis of 18s rDNA and *rbc*L sequences. *J Mol Evol* 1998;**47**:420–30.

Hodač L, Hallmann C, Spitzer K *et al*. Widespread green algae *Chlorella* and *Stichococcus* exhibit polar-temperate and tropical-temperate biogeography. *FEMS Microbiol Ecol* 2016;**92**:fiw122.

Hoham RW. New findings in the life history of the snow alga, *Chlainomonas rubra* (Stein et Brooke) comb. nov. (Chlorophyta, Volvocales). *Syesis* 1974;**7**:239–47.

Hoham RW, Roemer SC, Mullet JE. The life history and ecology of the snow alga *Chloromonas brevispina* comb. nov. (Chlorophyta, Volvocales). *Phycologia* 1979;**18**:55–70.

Hooker JD. 36. Red snow. *Edinb J Sci* 1825;**2**:184.

Ji M, Greening C, Vanwonterghem I *et al*. Atmospheric trace gases support primary production in Antarctic desert surface soil. *Nature* 2017;**552**:400–3.

Jombart T. *adegenet*: A R package for the multivariate analysis of genetic markers. *Bioinformatics* 2008;**24**:1403–5.

Jombart T, Pontier D, Dufour AB. Genetic markers in the playground of multivariate analysis. *Heredity* 2009;**102**:330–41.

Jombart T, Devillard S, Dufour AB *et al*. Revealing cryptic spatial patterns in genetic variability by a new multivariate method. *Heredity* 2008;**101**:92–103.

Jones HG, Pomeroy JW, Walker DA *et al*.(eds.) *Snow ecology. An interdisciplinary examination of snow-covered ecosystems*. Cambridge: Cambridge University Press, 2001; 378.

Kawecka B. Biology and ecology of snow algae 2. Formation of aplanospores in *Chlamydomonas nivalis* (Bauer) Wille (Chlorophyta, Volvocales). *Acta Hydrobiol* 1981;**23**:211–5.

Kobayashi Y, Fukushima H. On the red and green snow newly found in Japan II. *Bot Mag Tokyo* 1952;**65**:128–36.

Koetschan C, Förster F, Keller A *et al*. The ITS2 Database III-sequences and structures for phylogeny. *Nucleic Acids Res* 2010;**38**:D275–9.

Kol E. The snow and ice algae of Alaska. *Smithsonian Miscellaneous Collection* 1942;**101**:1–36.

Kol E. *Kryobiologie: Biologie und Limnologie des Schnees und Eises, I. Kryovegetation*. Die Binnengewässer Einzeldarstellungen aus der Limnologie und ihren Nachbargebieten Volume XXIV volume 24. Stuttgart: E. Schweizerbart'sche Verlagsbuchhandlung (Nägele u. Obermiller), 1968.

Ley R, Williams MW, Schmidt SK. Microbial population dynamics in an extreme environment: controlling factors in talus soils at 3750 m in the Colorado Rocky Mountains. *Biogeochemistry* 2004;**68**:313–35.

Leya T. Feldstudien und genetische Untersuchungen zur Kryophilie der Schneealgen Nordwestspitzbergens. *Berichte aus der Biologie*. Aachen: Shaker, 2004.

Leya T. *Die „Ross-Proben" von den Crimson Cliffs: Probe „MB_ES_1781c" aus der Ehrenberg Sammlung des Naturkundemuseums Berlin*. Berlin: Fraunhofer IBMT, 2008, 6.

Leya T, Müller T, Ling HU *et al*. Snow algae from north-western Spitsbergen (Svalbard). *Reports on Polar and Marine Research* 2004;**492**:46–54.

Leya T, Rahn A, Lütz C *et al*. Response of arctic snow and permafrost algae to high light and nitrogen stress by changes in pigment composition and applied aspects for biotechnology. *FEMS Microbiol Ecol* 2009;**67**:432–43.

Librado P, Rozas J. DnaSP v5: a software for comprehensive analysis of DNA polymorphism data. *Bioinformatics* 2009;**25**:1451–2.

Ling HU. Snow algae of the Windmill Islands, continental Antarctica: *Chlorosarcina antarctica* comb. nov. (Chlorophyceae, Chlorophyta) from pink snow, with discussion of *Chlorosarcina* and allied genera. *Phycologia* 2002;**41**:1–9.

Ling HU, Seppelt RD. Snow algae of the Windmill Islands, continental Antarctica. 2. *Chloromonas rubroleosa* sp. nov. (Volvocales, Chlorophyta), an alga of red snow. *Eur J Phycol* 1993;**28**:77–84.

Link DHF. *45./2. Coccophysium nivale. Handbuch zur Erkennung der nutzbarsten und am häufigsten vorkommenden Gewächse Drittel Teil*. Berlin: Haude und Spenersche Buchhandlung(S.J. Joseephy), 1833, 341–2.

Lu N, Wei D, Chen F *et al*. Lipidomic profiling reveals lipid regulation in the snow alga *Chlamydomonas nivalis* in response to nitrate or phosphate deprivation. *Process Biochem* 2012a;**48**:605–13.

Lu N, Wei D, Jiang X-L *et al*. Regulation of lipid metabolism in the snow alga *Chlamydomonas nivalis* in response to NaCl stress: An integrated analysis by cytomic and lipidomic approaches. *Process Biochem* 2012b;**47**:1163–70.

Lu N, Chen JH, Wei D *et al*. Global metabolic regulation of the snow alga *Chlamydomonas nivalis* in response to nitrate or phosphate deprivation by a metabolome profile analysis. *Int J Mol Sci* 2016;**17**:19.

Lutz S, Anesio AM, Raiswell R *et al*. The biogeography of red snow microbiomes and their role in melting arctic glaciers. *Nat Commun* 2016;**7**:11968.

Lütz-Meindl U, Lütz C. Analysis of element accumulation in cell wall attached and intracellular particles of snow algae by EELS and ESI. *Micron* 2006;**37**:452–8.

Marchant HJ. Snow algae from the Australian Snowy Mountains. *Phycologia* 1982;**21**:178–84.

Marshall WA. Biological particles over Antarctica. *Nature* 1996;**383**:680.

Mataloni G, Tesolín G. A preliminary survey of cryobiontic algal communities from Cierva Point (Antarctic Peninsula). *Antarct Sci* 1997;**9**:250–8.

Matsuzaki R, Hara Y, Nozaki H. A taxonomic revision of *Chloromonas reticulata* (Volvocales, Chlorophyceae), the type species of the genus *Chloromonas*, based on multigene phylogeny and comparative light and electron microscopy. *Phycologia* 2012;**51**:74–85.

Matsuzaki R, Nozaki H, Kawachi M. Taxonomic revision of *Chloromonas nivalis* (Volvocales, Chlorophyceae) strains, with the new description of two snow-inhabiting *Chloromonas* species. *PLoS One* 2018;**13**:e0193603.

Matsuzaki R, Nozaki H, Takeuchi N *et al*. Taxonomic re-examination of "*Chloromonas nivalis* (Volvocales, Chlorophyceae) zygotes" from Japan and description of *C. muramotoi* sp. nov. *PLoS One* 2019;**14**:e0210986.

Mazumdar N, Gopalakrishnan KK, Visnovsky G *et al*. A novel alpine species of *Haematococcus* (Chlamydomonadales: Chlorophyta) from New Zealand. *N Z J Bot* 2018;**56**:216–26.

Muramoto K, Nakada T, Shitara T *et al*. Re-examination of the snow algal species *Chloromonas miwae* (Fukushima) Muramoto et al., comb. nov. (Volvocales, Chlorophyceae) from Japan, based on molecular phylogeny and cultured material. *Eur J Phycol* 2010;**45**:27–37.

Meneghini G. Monographia Nostochinearum italicarum addito specimine de Rivulariis. *Memorie della Reale Accademia delle Scienze di Torino, ser 2* 1843;**5**:1–143 pls I-XVII.

Mosser JL, Mosser AG, Brock TD. Photosynthesis in the snow: The alga *Chlamydomonas nivalis* (Chlorophyceae). *J Phycol* 1977;**13**:22–7.

Müller T, Leya T, Fuhr G. Persistent snow algal fields in Spitsbergen: Field observations and a hypothesis about the annual cell circulation. *Arct Antarct Alp Res* 2001;**33**:42–51.

Müller T, Bleiß W, Martin C-D *et al*. Snow algae from northwest Svalbard: their identification, distribution, pigment and nutrient content. *Polar Biol* 1998;**20**:14–32.

Nagai S, Lian C, Yamaguchi S *et al*. Microsatellite markers reveal population genetic structure of the toxic dinoflagellate *Alexandrium tamarense* (Dinophyceae) in Japanese coastal waters. *J Phycol* 2007;**43**:43–54.

N.N. *Captain Sir John Ross has brought from Baffin's Bay a Quantity of Red Snow*. London: London Times, 1818.

Nakada T, Ota S. What is the correct name for the type of *Haematococcus* Flot. (Volvocales, Chlorophyceae)? *Taxon* 2016;**65**:343–8.

Nedbalová L, Mihál M, Kvíderová J *et al*. Identity, ecology and ecophysiology of planktic green algae dominating in ice-covered lakes on James Ross Island (northeastern Antarctic Peninsula). *Extremophiles* 2017;**21**:187–200.

Novakovskaya IV, Patova EN, Boldina ON *et al*. Molecular phylogenetic analyses, ecology and morphological characteristics of *Chloromonas reticulata* (Goroschankin) Gobi which causes red blooming of snow in the subpolar Urals. *Cryptogam, Algol* 2018;**39**:199–213.

Novis PM. Ecology of the snow alga *Chlainomonas kolii* (Chlamydomonadales, Chlorophyta) in New Zealand. *Phycologia* 2002;**41**:280–92.

Novis PM, Visnovsky G. Novel alpine algae from New Zealand: Chlorophyta. *Phytotaxa* 2012;**39**:1–30.

Novis PM, Hoham RW, Beer T *et al*. Two snow species of the quadriflagellate green alga *Chlainomonas* (Chlorophyta, Volvocales): Ultrastructure and phylogenetic position within the *Chloromonas* clade. *J Phycol* 2008;**44**:1001–12.

Nozaki H, Onishi K, Morita E. Differences in pyrenoid morphology are correlated with differences in the rbcL genes of members of the *Chloromonas* lineage (Volvocales, Chlorophyceae). *J Mol Evol* 2002;**55**:414–30.

Persoon CH, Göttingen. *Synopsis Methodica Fungorum*. 1801;**1**:214.

Perty M. Zur Kenntnis kleinster Lebensformen. *Bern* 1852:1–228.

Posada D. jModelTest: phylogenetic model averaging. *Mol Biol Evol* 2008;**25**:1253–6.

Procházková L, Remias D, Řezanka T *et al*. *Chloromonas nivalis* subsp. *tatrae*, subsp. nov. (Chlamydomonadales, Chlorophyta): re-examination of a snow alga from the High Tatra Mountains (Slovakia). *Fottea* 2018a;**18**:1–18.

Procházková L, Remias D, Holzinger A *et al*. Ecophysiological and morphological comparison of two populations of *Chlainomonas* sp. (Chlorophyta) causing red snow on ice-covered lakes in the High Tatras and Austrian Alps. *Eur J Phycol* 2018b;**53**:230–43.

Pröschold T, Marin B, Schlösser UG *et al*. Molecular phylogeny and taxonomic revision of *Chlamydomonas* (Chlorophyta). I. Emendation of *Chlamydomonas* Ehrenberg and *Chloromonas* Gobi, and description of *Oogamochlamys* gen. nov. and *Lobochlamys* gen. nov. *Protist* 2001;**152**:265–300.

Remias D. Cell Structure and Physiology of Alpine Snow and Ice Algae. In: Lütz C (ed.) *Plants in Alpine Regions: Cell Physiology of Adaptation and Survival Strategies*. Wien: Springer, 2012, 175–85.

Remias D, Lütz-Meindl U, Lütz C. Photosynthesis, pigments and ultrastructure of the alpine snow alga *Chlamydomonas nivalis*. *Eur J Phycol* 2005;**40**:259–68.

Remias D, Karsten U, Lütz C *et al*. Physiological and morphological processes in the Alpine snow alga *Chloromonas nivalis* (Chlorophyceae) during cyst formation. *Protoplasma* 2010;**243**:73–86.

Remias D, Wastian H, Lütz C *et al*. Insights into the biology and phylogeny of *Chloromonas polyptera* (Chlorophyta), an alga causing orange snow in Maritime Antarctica. *Antarct Sci* 2013;**25**:648–56.

Remias D, Pichrtová M, Pangratz M *et al*. Ecophysiology, secondary pigments and ultrastructure of *Chlainomonas* sp. (Chlorophyta) from the European Alps compared with *Chlamydomonas nivalis* forming red snow. *FEMS Microbiol Ecol* 2016;**92**:fiw030.

Ross J. *A Voyage of Discovery, Made Under the order of the Admirality, in His Majesty's Ships Isabella and Alexander for the Purpose of Exploring Baffin's Bay, and Inquiring into the Probability of a North-West Passage*. London: John Murray, 1819.

Ross J (ed.) *Entdeckungsreise unter den Befehlen der Britischen Admiraltät mit den Königlichen Schiffen Isabella und Alexander um Baffins-Bay auszuforschen und die Möglichkeit einer nordwestlichen Durchfahrt zu Untersuchen*. Leipzig: Friedrich Fleischer, 1820.

Sattler B, Remias D, Lütz C *et al.* Leben auf Schnee und Eis. In: Erschbamer B Koch EM (eds.) *Glaziale und periglaziale Lebensräume im Raum Obergurgl*. Innsbruck: Innsbruck University Press iup, 2010.

Schlichting HE, Jr. The importance of airborne algae and Protozoa. *J Air Pollut Control Assoc* 1969;**19**:946–51.

Schultz J, Wolf M. ITS2 sequence-structure analysis in phylogenetics: A how-to manual for molecular systematics. *Mol Phylogen Evol* 2009;**52**:520–3.

Segawa T, Matsuzaki R, Takeuchi N *et al.* Bipolar dispersal of red-snow algae. *Nat Commun* 2018;**9**:3094.

Seibel PN, Müller T, Dandekar T *et al.* Synchronous visual analysis and editing of RNA sequence and secondary structure alignments using 4SALE. *BMC Res Notes* 2008;**1**:91.

Seibel PN, Müller T, Dandekar T *et al.* 4SALE - A tool for synchronous RNA sequence and secondary structure alignment and editing. *BMC Bioinformatics* 2006;**7**:498.

Shuttleworth RJ. Upon the colouring matter of red snow. *The Edinburgh New Philosophical Journal* 1840a;**29**:54–64 (with 1 coloured plate).

Shuttleworth RJ. Nouvelles observations sur la matière colorant de la neige rouge. 1840b;**25**, Geneva.

Škaloud P, Rindi F. Ecological differentiation of cryptic species within an asexual protist morphospecies: a case study of filamentous green alga *Klebsormidium* (Streptophyta). *J Eukaryot Microbiol* 2013;**60**:350–62.

Škaloud P, Steinová J, Řídká T *et al.* Assembling the challenging puzzle of algal biodiversity: species delimitation within the genus *Asterochloris* (Trebouxiophyceae, Chlorophyta). *J Phycol* 2015;**51**:507–27.

Sommerfelt SC. Om den røde Sne, eller *Sphærella nivalis* Sommerf., *Uredo nivalis* Auct. *Mag Nat videnskab* 1824;**4**:249–53.

Spijkerman E, Wacker A, Weithoff G *et al.* Elemental and fatty acid composition of snow algae in Arctic habitats. *Front Microbiol* 2012;**3**:380.

Sprengel C. *Coccochloris nivalis* Spreng. *Syst Veg* 1827;**4**:373.

Stein JR, Amundsen CC. Studies on snow algae and fungi from the front range of Colorado. *Can J Bot* 1967;**45**:2033–45.

Stibal M, Elster J, Šabacká M *et al.* Seasonal and diel changes in photosynthetic activity of the snow alga *Chlamydomonas nivalis* (Chlorophyceae) from Svalbard determined by pulse amplitude modulation fluorometry. *FEMS Microbiol Ecol* 2007;**59**:265–73.

Sutton EA. The physiology and life histories of selected cryophytes of the Pacific Northwest *Department of Oceanography* volume PhD. Corvallis, OR: Oregon State University, 1970, 98.

Terashima M, Umezawa K, Mori S *et al.* Microbial community analysis of colored snow from an alpine snowfield in northern Japan reveals the prevalence of betaproteobacteria with snow algae. *Front Microbiol* 2017;**8**:1481.

Thomas WH, Broady PA. Distribution of coloured snow and associated algal genera in New Zealand. *N Z J Bot* 1997;**35**:113–7.

VanWinkle-Swift KP, Rickoll WL. The zygospore wall of *Chlamydomonas monoica* (Chlorophyceae): morphogenesis and evidence for the presence of sporopollenin. *J Phycol* 2008;**33**:655–65.

Vogt C. Neige rouge. In: Desor E (ed.) *Excursions et séjours dans les glaciers et les hautes régions des Alpes, de M Agassiz et de ses compagnons de voyage*. Neuchatel and Paris, 1844, 215–24(16; pl. 1: fig. 1-5 (as '*Discerea nivalis*').

Vukić J, Ulqini D, Šanda R. Occurrence of *Knipowitschia goerneri* Ahnelt, 1991 (Gobiidae) in southern Albania confirmed with molecular tools. *J Appl Ichthyol* 2017;**33**:284–90.

Wayama M, Ota S, Matsuura H *et al.* Three-dimensional ultrastructural study of oil and astaxanthin accumulation during encystment in the green alga *Haematococcus pluvialis*. *PLoS One* 2013;**8**:e53618.

Wilkinson DM, Koumoutsaris S, Mitchell EAD *et al.* Modelling the effect of size on the aerial dispersal of microorganism. *J Biogeogr* 2012;**39**:89–97.

Wille N. Algologische Notizen IX-XIV. *Nyt Magazin for Naturvidenskaberne* 1903;**41**:89–185.

Wrangel FA. Microscopiska och Physiologiska Undersökningar rörande utvecklingen af *Lepraria Kermesina* och dess likhet med den sa kallade röda Snön. Tilläg till Anmärkningarne rörande *Byssus Jolithus* Linn. *Kongl Vetenskaps-Akademiens Handlingar för år 1823, Stockholm* 1823;**1**:71–95.

Žárský V, Kalina T, Sulek J. Notes on the sexual reproduction of *Chlamydomonas geitleri* Ettl. *Arch Protistenkd* 1985;**130**:343–53.

Zuker M. Mfold web server for nucleic acid folding and hybridization prediction. *Nucleic Acids Res* 2003;**31**:3406–15.